Review article

Fenfen Zheng*, Weiwei Xiong, Shasha Sun, Penghui Zhang and Jun Jie Zhu*

Recent advances in drug release monitoring

https://doi.org/10.1515/nanoph-2018-0219
Received December 14, 2018; revised February 1, 2019; accepted February 2, 2019

Abstract: Monitoring drug release *in vitro* and *in vivo* is of paramount importance to accurately locate diseased tissues, avoid inappropriate drug dosage, and improve therapeutic efficiency. In this regard, it is promising to develop strategies for real-time monitoring of drug release inside targeted cells or even in living bodies. Thus far, many multi-functional drug delivery systems constructed by a variety of building blocks, such as organic molecules, polymeric nanoparticles, micelles, and inorganic nanoparticles, have been developed for drug release monitoring. Especially, with the advancements in imaging modalities relating to nanomaterials, there has been an increasing focus on the use of non-invasive imaging techniques for monitoring drug release and drug efficacy in recent years. In this review, we introduce the application of fluorescence imaging, magnetic resonance imaging (MRI), surface-enhanced Raman scattering (SERS), and multi-mode imaging in monitoring drug release, involving a variety of nanomaterials such as organic or inorganic nanoparticles as imaging agents; their design principles are also elaborated. Among these, a special emphasis is placed on fluorescence-based drug release monitoring strategies, followed by a brief overview of MRI, SERS, and multi-mode imaging-based strategies. In the end, the challenges and prospects of drug release monitoring are also discussed.

***Corresponding authors: Fenfen Zheng,** School of Environmental and Chemical Engineering, Jiangsu University of Science and Technology, Zhenjiang, Jiangsu 212003, P.R. China, e-mail: fenfenzheng1108@126.com; and **Jun Jie Zhu,** State Key Laboratory of Analytical for Life Science, School of Chemistry and Chemical Engineering, Nanjing University, Nanjing, Jiangsu 210023, P.R. China, e-mail: jjzhu@nju.edu.cn. https://orcid.org/0000-0002-8201-1285
Weiwei Xiong and Shasha Sun: School of Environmental and Chemical Engineering, Jiangsu University of Science and Technology, Zhenjiang, Jiangsu 212003, P.R. China
Penghui Zhang: The Key Laboratory of Biomedical Information Engineering of Ministry of Education, School of Life Science and Technology, Bioinspired Engineering and Biomechanics Center (BEBC), Xi'an Jiaotong University, Xi'an, China

Keywords: drug delivery system; drug release monitoring; fluorescence imaging; MRI; SERS; multi-mode imaging; nanomaterials.

1 Introduction

In the realm of inoperable cancer-based therapies, a number of therapeutics (e.g. drugs, antibodies, gene strands) are highly recommended for inhibiting tumor growth and preventing recurrence. However, due to the poor selectivity and high toxicity, their severe side effects to normal organs and limited therapeutic efficacy to tumor tissues have hindered their clinical usage for cancer therapy [1–4]. In recent years, the flourishing development of chemistry and material science has brought about a burst of research activities in drug delivery systems (DDSs), which are aimed to address the biomedical challenges in traditional medicine. To achieve site-specific drug delivery for controllable pharmacokinetics and biodistribution, a variety of targeted DDSs were designed. The most common strategy to achieve high targeting efficiency is based on passive targeting, which involves the enhanced permeability and retention (EPR) effect caused by the leaky vasculature and dysfunctional lymphatic drainage of many solid tumors [5, 6], usually resulting in the high accumulation of macromolecules as well as nanoparticles with a diameter of 20–500 nm in the tumor tissue [7, 8]. This targeting strategy is universal and enables the DDS to treat a wide range of solid tumors. Differently, active targeting relies on specific interactions between membrane-bound receptors (e.g. proteins, glycoproteins, and lipoproteins) on tumor cells and corresponding ligands (e.g. saccharides, lectins, antibodies and antibody fragments, peptides, nucleotides, enzymes, or enzyme inhibitors) on the DDS surface. The targeting ligands can guide the delivery vehicle to the desired action site and avoid non-specific uptake by healthy cells and tissues [9, 10]. The active targeting strategies are not only selective and effective against solid tumors, but they also show potent efficacy to leukemia and circulating tumor cells that are less sensitive to passively targeted DDSs. To further enhance the specific drug release at the tumor site and improve the therapeutic efficacy, controllable

DDSs were developed to respond to specific stimuli [11, 12], including exogenous triggers (e.g. temperature [13], magnetic field [14, 15], ultrasound [16], light [17, 18], electric pulses [19, 20], etc.) and endogenous triggers (acidic pH [21, 22], enzyme [23, 24] or redox species [25, 26], etc.), making it possible to deliver drugs in spatial-, temporal- and dosage-controlled fashions. However, in most cases, crucial data of *in situ* and real-time drug release from these DDSs in living cells or *in vivo* cannot be directly obtained, and the unknown actual drug concentrations at the focus have perplexed doctors. To overcome these hurdles, multi-functional DDSs, capable of targeting tumor cells, controlling drug release, and real-time monitoring, are being developed, which is absolutely critical when an on-demand dose of drug is needed to reach the pathological region of interest without damaging normal tissues.

As is known, except for serving as promising scaffolds for drug loading, most organic and inorganic nanomaterials with unique physicochemical properties have been applied as imaging contrast agents for early disease detection and treatment monitoring [27–29]. After being integrated with a tracking method, the multi-functional DDS can not only image the targeted tissues but also monitor the drug release kinetics in a real-time and long-term fashion. Considering the limitations of invasive imaging in clinical treatment, non-invasive imaging techniques, such as fluorescence imaging, magnetic resonance imaging (MRI), and surface-enhanced Raman scattering (SERS) imaging, are well developed for monitoring drug delivery, drug release, and therapeutic efficacy [30–33]. Moreover, to optimally integrate the advantages of different imaging modes in one DDS, multi-mode imaging (allowing more than one imaging mode to act synergistically) was also established. These real-time systems for tracking where, when, and how drugs are delivered and released may provide an in-depth insight into the drug uptake process, pharmacokinetics, biodistribution, local distribution at the target site, kinetics of drug release, and therapeutic efficacy. In turn, this spatiotemporal information on the DDSs and drugs also offers guidance for the development and optimization of drug therapy in terms of DDS engineering, drug release modalities, and administration approaches.

In this review, we provide an overview of recent advances in drug release monitoring followed by highlights of four imaging strategies in the field of drug release monitoring: fluorescence imaging, MRI, SERS, and multi-mode imaging. In each case, we present the merits of the imaging technique as well as the advances of nanomaterials that enable the technique to overcome the barriers for drug release monitoring and effective drug therapy. Among them, we mainly introduce the development of the fluorescence-based drug release monitoring strategies and briefly outline the MRI, SERS, and multi-mode imaging-based strategies. We hope that this review will provide the most updated summary of the design, performance, and application of drug release monitoring strategies.

2 Fluorescence-based drug release monitoring strategies

Fluorescence is produced by the radiative transition of excitation energy after light absorption, which is fast, with a lifetime decay in nanoseconds. Among the biomedical imaging technologies, fluorescence imaging can timely reflect the biodistribution and pharmacokinetics of DDSs due to its real-time, non-invasive, highly sensitive, and radiation-free features [34–36]. To track drug transportation and release *in vitro* and *in vivo*, efforts have been devoted to couple fluorescent agents to the drug release event in a delivery system, and real-time information about the release process can be obtained using non-invasive fluorescence imaging techniques. Particularly, among various fluorescence imaging systems, near-infrared (NIR) fluorescence imaging has become the overwhelming choice to visualize species of interest *in vivo*, because NIR protons can deeply penetrate tissue and skin with minimal background interference [37, 38]. Moreover, multiple fluorophores can be imaged in the same cell or animal, facilitating the development of multi-channel imaging for tracking multiple biological events simultaneously. As the performance of fluorescence-based drug release monitoring strategies greatly depend on the optical property of imaging agents as well as the nanocarriers, in this section, various organic or inorganic fluorescent agents and carrier materials are summarized and discussed.

2.1 Prodrug-based drug release monitoring

Over the past decades, prodrugs were developed as an effective approach for cancer therapy. This strategy provides great possibilities to overcome various drawbacks of drug molecules, such as poor solubility, systemic instability, and lack of cancer specificity. Recently, theranostic prodrugs, which exhibit the dual purpose of diagnosis and therapy, are emerging as a promising technology in biomedicine. The theranostic prodrugs can covalently bind with fluorophores as fluorescent reporters to monitor the

drug release process, and the fluorescence signals could be of great benefit to evaluate their therapeutic effect, pharmacodynamics, and activation mechanism. These prodrugs enable researchers to know when, where, and how the active drug molecules are delivered, and can even semi-quantitatively detect the release of active drugs in a non-invasive manner.

By coupling latent fluorophores to the drug molecules with an activatable linker, real-time information about the drug release process can be obtained by using non-invasive fluorescence detection techniques. For instance, Weinstain et al. [39] reported a DDS for real-time monitoring drug release *in vitro* by using a coumarin-based linker. In this system, the drug release event occurring in the cytoplasm of human umbilical vein endothelial cells was observed directly with the aid of confocal microscopy, and the amount of released drug was calculated by quantifying the emitted fluorescence, allowing the prediction of therapeutic effect and potential side effects. Similarly, Bazylevich et al. [40] developed a fluorescein-based prodrug by conjugating free phenolic hydroxyl of fluorescein chemosensor to the hydroxyl group of the drugs for monitoring drug release. Hu and Zeng [41] designed a theranostic prodrug, composed of an anti-cancer drug camptothecin (CPT), a cleavable linker based on disulfide bonds, and a fluorophore naphthalimide derivative, and detected the drug release *via* the fluorescence resonance energy transfer (FRET) mechanism. The FRET occurring between CPT (energy donor) and naphthalimide (energy receptor) was interrupted by the high concentration of intracellular glutathione (GSH), thus achieving dual fluorescence response and specific release of CPT. Liu et al. [42] reported a ratiometric theranostic prodrug consisting of boron dipyrromethene, therapeutic drug CPT, and a long flexible disulfide linker. Once treated with dithiothreitol, the disulfide bond was cleaved and CPT was released, resulting in enhanced blue and green fluorescence emissions. The changes of the fluorescence ratio over time provided the opportunity for the real-time monitoring of drug release at cellular levels. DT-diaphorase, an enzyme overexpressed in some malignant tumors, can be exploited to catalyze the reduction of quinine propionic acid moiety incorporated into prodrug, which could be utilized for concomitant drug release imaging and cancer chemotherapy [43, 44]. In order to monitor drug release more accurately and understand pharmacological mechanisms better, Kong et al. [45] developed a dual turn-on fluorescence based controlled release system (CDox), in which doxorubicin (Dox) and fluorescent dye (CH) are conjugated by a pH-responsive cleavable hydrazone linker. The C=N isomerization and N-N free rotation efficiently quenched the fluorescence of CH and Dox in the CDox complex. When activated under acidic conditions, CDox was hydrolyzed to release Dox and CH, resulting in dual turn-on signals with emission peaks at 595 and 488 nm, respectively. Using this system, two-photon fluorescence imaging of CDox in living tumor tissues was successfully performed by high-definition three-dimensional (3D) imaging.

NIR fluorophores are often used as fluorescent reporters for *in vivo* drug release monitoring because NIR photons can deeply penetrate the skin and underlying tissue with minimal damage to the biological samples and with low background interference. Zhang et al. [46] reported a real-time drug-reporting conjugate (CPT-SS-CyN), composed of a NIR fluorescent cyanine-amine dye (CyN), a disulfide linker, and a model therapeutic drug (CPT) (Figure 1A). Likewise, treatment with dithiothreitol induces cleavage of the disulfide bond, resulting in the release of NIR dye and the drug CPT. The released CyN has an emission wavelength (760 nm) that is significantly different from that of CPT-SS-CyN (820 nm), enabling easy detection and monitoring of drug release. A linear relationship of the fluorescence intensity at 760 nm versus the amount of released CPT was observed, enabling quantitative monitoring of drug release in live cells and semi-quantitative monitoring in live animals in a real-time and non-invasive manner. Additionally, a NIR fluorophore, dicyanomethylene-4H-pyran derivative (DCM), was conjugated with anti-cancer CPT through a disulfide linker (DCM-S-CPT), which can be cleaved by the overexpressed intracellular GSH, making the drug activation and fluorescence turn on concomitantly. Furthermore, DCM-S-CPT has been successfully utilized for assessing drug release and cancer therapeutic efficacy by analyzing NIR fluorescence *in vivo* and *in situ* (Figure 1B) [47].

The fluorescent signals of single-channel fluorescent theranostic prodrugs were usually unobservable before drug release; therefore, it is difficult to simultaneously monitor their biodistribution and drug release in spatiotemporal mode. The metabolism kinetics of prodrugs in a certain organ or tissue becomes a blind spot, which is a critical obstacle in the precise diagnosis and chemotherapy. The development of two-color imaging systems with two-channel fluorescence that can distinguish the signals before and after drug release has opened a window to overcome this hurdle. Liu et al. [49] reported a novel light-activated cleavable prodrug comprising a photoremovable coumarinyl, the anti-cancer drug CPT, a cleavable linker, and the NIR fluorescent dye DCM. In this prodrug, owing to FRET, the fluorescence of coumarinyl and CPT is completely quenched while the DCM moiety shows red emission, which

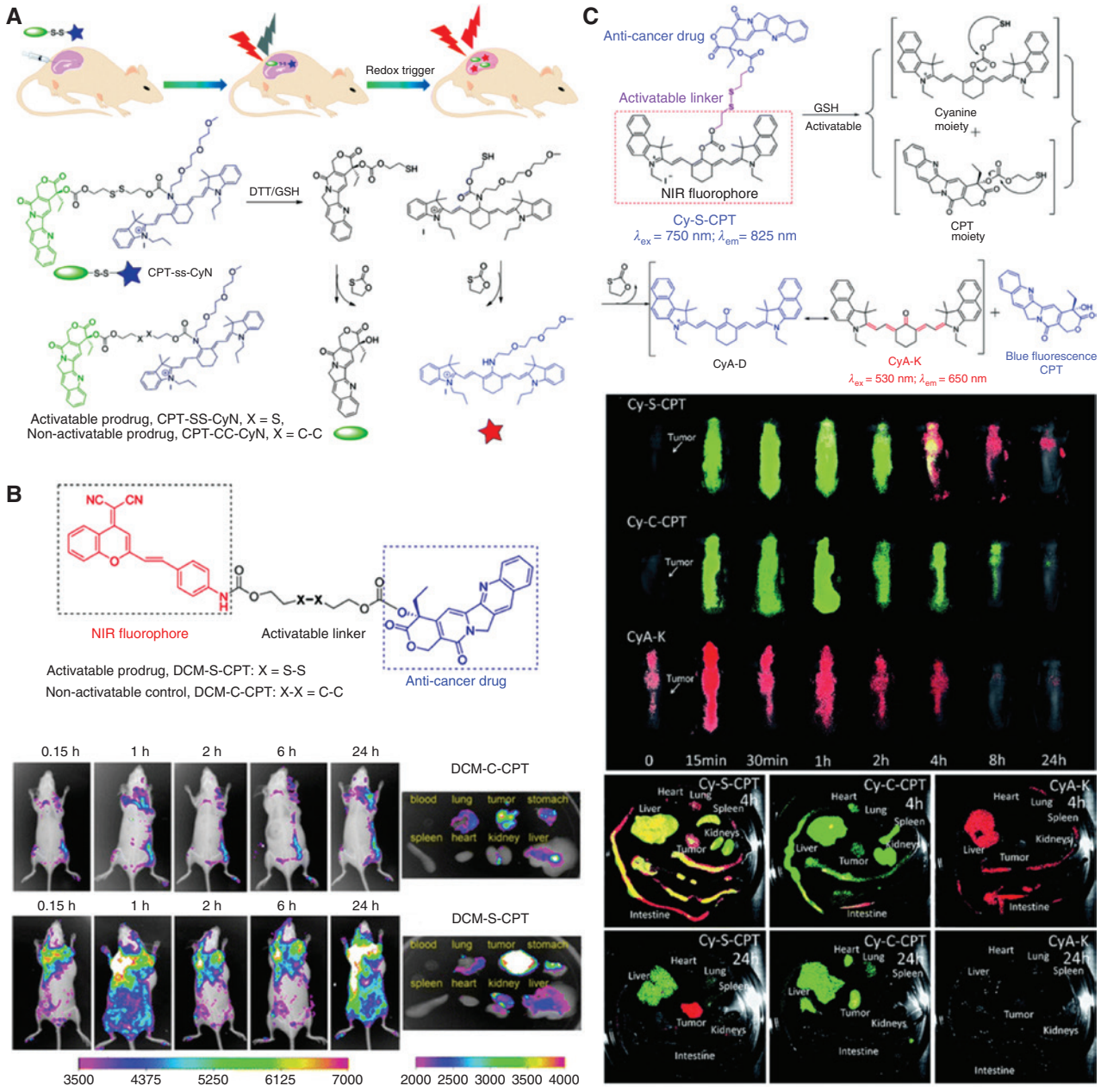

Figure 1: Monitoring drug release by fluorescent prodrugs.
(A) Schematic illustration of real-time tracking of active drug release *in vivo* and proposed mechanism for concurrent NIR/CPT release from CPT-SS-CyN triggered by DTT/GSH. (Adapted from Ref. [46].) (B) Chemical structures of activatable prodrug DCM-S-CPT and non-activatable control DCM-C-CPT. Also, *in vivo* imaging of tumor-bearing mice at various times (0.15, 1, 2, 6, and 24 h) after intravenous injection and fluorescence images of the internal organs after anatomy. The color bars correspond to the detected fluorescence intensity. (Adapted from Ref. [47].) (C) Proposed mechanism in CPT activation and fluorescence variation of the prodrug Cy-S-CPT by the treatment of GSH. Also, *in vivo* and *ex vivo* bioimaging of tumor-bearing mice at various times (0.25, 0.5, 1, 2, 4, 8, and 24 h) after intravenous injection of the different prodrugs. Note that the green signal represents the fluorescence from the intact prodrugs (λ_{ex} = 750 nm, λ_{em} = 825 nm) for tracking the prodrug biodistribution, whereas red signal represents the fluorescence from CyA-K (λ_{ex} = 530 nm, λ_{em} = 650 nm) for tracking the location of drug activation. Yellow represents the coexistence of prodrug and drug release. (Adapted from Ref. [48].)

can be used to visualize the drug localization before irradiation. Upon one- or two-photon irradiation, the prodrug releases active CPT, and the release process is monitored *via* the change in the FRET process. Ye et al. [48] presented a dual-channel NIR activatable theranostic prodrug, in which the CPT was linked to a NIR cyanine dye *via* a disulfide linkage (Cy-S-CPT) (Figure 1C). The cleavage of the disulfide bond by endogenous GSH activated the anti-cancer drug

and induced a remarkable fluorescence shift from 825 to 650 nm, thereby providing dual fluorescent channels to real-time track the prodrug biodistribution and activation *in vivo*. As demonstrated, the prodrug was activated in all organs, particularly in the liver after an intravenous injection, and achieved predominant accumulation and activation in tumors at 24 h after injection.

In addition, such a dual-channel fluorescence strategy can also be applied to monitor drug release and evaluate therapeutic efficacy simultaneously. As is known, the activity of intracellular apoptotic proteases such as caspase-3 can reflect the degree of cell apoptosis, which is highly related to the therapeutic efficacy. Based on these, Li et al. [50] developed a versatile prodrug for real-time drug release monitoring and *in situ* therapeutic efficacy evaluation. In this system, the fluorescence of both 5(6)-carboxylfluorescein and Dox was quenched by 4-(dimethylaminoazo)benzene-4-carboxylic acid *via* FRET. On the one hand, the acid-mediated Dox release from the prodrug was real-time monitored according to the increase of liberated Dox fluorescence. On the other hand, Dox-induced cell apoptosis was *in situ* assessed by the fluorescence recovery of 5(6)-carboxylfluorescein, resulting from the caspase-3-mediated cleavage of the Asp-Glu-Val-Asp peptide. Through this cascaded imaging strategy, the drug release and consequent cell apoptosis were real-time monitored, enabling the *in situ* detection of pharmacokinetics and treatment response.

2.2 Macromolecule-based drug release monitoring

As driven by the exponentially increasing demand for "intelligent" materials, responsive polymers, polymeric nanoparticles, micelles, and other macromolecules that are capable of adapting to changes in local environment have attracted tremendous interest in recent years. These materials with autofluorescence or labeled fluorescence have been exploited for controlled drug release with real-time tracking ability due to their low cytotoxicity and good biocompatibility.

Most of the anti-cancer drugs have little aqueous solubility and permeability. One common way to deliver hydrophobic drugs to the target site is to construct a prodrug that can create a synthetic analogue with higher hydrophilicity by modification. However, even with this approach, it is still difficult to extend the circulation time of drugs in the blood and to suppress the fast renal excretion, thus lowering the curative effect. One way to solve this problem is incorporating the drug molecules with polymer nanoparticles. Wu et al. [47] and Ye et al. [48] demonstrated that loading the prodrug into polymeric nanoparticles could significantly improve the therapeutic efficacy and lower the side effects owing to the EPR effect. Another example is perylene, which can act as an efficient phototrigger for carboxylic acids and alcohols in aqueous media under visible light irradiation. The perylene molecules can form nanoparticles with different sizes by the re-precipitation method, and the perylene nanoparticles show different spectral properties compared with the free perylene molecules. Jana et al. [51, 52] reported chlorambucil-conjugated perylene organic nanoparticles as single-component photoresponsive nanocarriers for controlling and monitoring drug release. In these systems, perylene nanoparticles performed four roles: (i) nanocarriers for drug delivery, (ii) phototriggers for drug release, (iii) fluorescent chromophores for cell imaging, and (iv) detectors for real time-monitoring of drug release.

Drug molecules can also conjugate with polymer nanocarriers to improve their efficacy and toxicity. The conjugated drugs are typically inactive in the polymer nanocarriers, and the triggered release will recover their therapeutic activity. To monitor the drug release in the polymer-drug conjugates, Shiran et al. [53] designed two N-(2-hydroxypropyl) methacrylamide co-polymer-based systems that were complementary to one theranostic nanomedicine consisting of self-quenched Cy5 as a reporter probe and paclitaxel as an anti-cancer agent. The established co-polymer systems enabled site-specific release upon enzymatic degradation in cathepsin B-overexpressed breast cancer cells, and the release of paclitaxel occurred concomitantly with the activation of Cy5 to the turn-on state. Apart from conjugating additional moieties for nanoparticle assembly, some drug molecules can self-assemble into nanoparticles for delivery. Zhang et al. [54] developed a self-carried curcumin nanodrug for highly effective cancer therapy *in vitro* and *in vivo* with real-time monitoring of drug release. Curcumin has different fluorescence characteristics in its molecular ("on" state, strong green fluorescence) and solid ("off" state, no emission because of intermolecular aggregation) forms, which was exploited in this study for monitoring the release of curcumin molecules ("on") from drug nanoparticles ("off") upon cell internalization.

Polymer nanoassemblies, such as polymer micelles, polymer vesicles, and polyionic complexes, are commonly created from self-assembling or cross-linked co-polymers. They are typically engineered to have a hydrophobic core to entrap drugs with low solubility and an enveloped hydrophilic shell to protect the drugs from precipitation, degradation, or non-specific binding to plasma proteins. By virtue of physically encapsulated or covalently linked

fluorophores, polymeric nanoassemblies have been extensively explored for tracing the biodistribution of nanocarriers and monitoring the drug release. For example, a series of fluorescent polymeric micelles have been constructed by self-assembly of two amphiphilic co-polymers with fluorescent moieties based on different fluorine derivatives. The drug release from these polymeric micelles could be monitored by the on/off of FRET from micelles to drugs [55]. Specifically, the modulating environment of some polymer nanoparticle cores, such as hydrophobicity or pH sensitivity, can control their fluorescence property. By tethering hydrophilic polymer chains (poly(ethylene glycol), PEG) onto a single polymer backbone (branched poly[ethylene imine], PEI) while modifying the core of the nanoassemblies with lipophilic pendant (palmitate, PAL) to modulate fluorochromism of Nile blue (NB), two types of polymer nanoassemblies were synthesized: PEG-PEI-NB (2PN) and PEG-PEI-PAL-NB (3PN) [56]. 2PN has ionizable moieties in the core that can attract water and quench NB fluorescence, while 3PN has a hydrophobic core modified with PAL to increase entrapment of hydrophobic anti-cancer drugs. Therefore, fluorescence intensity increased upon addition of hydrophobic drugs or exposure to acidic environments. These two polymer nanoassemblies were used to monitor the amount of drug remaining in the hydrophobic core in real time and detect metastatic tumors in a tissue pH-dependent manner. Aibani et al. [57] exploited differences in the hydrophobic/hydrophilic balance between two isomers, spiropyran and merocyanine, to mediate drug release from a polymer micelle. The stable spiropyran with closed hydrophobic four-ring system preferentially favors a non-polar environment, whereas light irradiation can convert to its zwittrionic merocyanine counterpart with open ring, which prefers a more hydrophilic environment. In addition, the drug was quantified using a FRET pair between spiropyran-merocyanine photochromic dyad and co-encapsulated boron dipyrromethene fluorophore. Therefore, this DDS based on polymer micelles not only is capable of releasing cargo under light, but also provides a real-time analysis of unreleased cargo.

The aggregation-induced emission (AIE) molecules, such as tetraphenylethene (TPE), triphenylethene, and siloles, commonly show no emission in dispersed solution due to the decaying of the excited energy *via* intramolecular rotations, while they exhibit high emission at the aggregated state because of the restricted intramolecular rotations. Such AIE phenomena can also be observed when the AIE molecules are aggregated in body fluids or in solid state, which favors cell imaging, chemical sensors, and investigating drug delivery mechanisms. For instance, AIE micelles prepared by conjugation of TPE with PEG were used as both nanocarriers to deliver anti-cancer drug and intracellular imaging probe to track their locations. Liow et al. [58] constructed a thermogelling co-polymer, poly(PEG/PPG/TPE urethane), consisting of hydrophilic PEG segment, hydrophobic poly(propylene glycol) (PPG) segment, and TPE units with AIE character (Figure 2A). As the AIE of the AIE thermogel is highly dependent on the Dox concentration and temperature, the drug release status and the erosion condition of the matrix can be revealed. Similarly, the PNIPAM thermogel can combine with LaF_3:Eu^{3+} nanocrystals by surface-initiated living radical polymerization [61]. The fluorescence properties and drug release behaviors in the core-shell LaF_3:Eu^{3+} nanocrystals/PNIPAM nanogels are highly related to the temperature. The fluorescence intensity of the nanogels increases gradually with the drug release.

Further, coordination polymers comprising organic ligands and metal ions can also be used for efficient monitoring of drug release in tumors. Fe^{3+} and polyphenol gallic acid can form a polygonal nanoscale coordination polymer with extremely high Dox loading efficacy (up to 48.3%) in aqueous solution, which exhibits potent antitumor effect [62]. *In vitro* studies demonstrated that the Dox fluorescence was efficiently quenched once loaded on the coordination polymer. The acidic microenvironment in lysosome could trigger Dox release and fluorescence recovery simultaneously, leading to real-time monitoring of drug release in tumor cells. The biocompatible dipeptide molecules (tryptophan-phenylalanine) could also coordinate with Zn^{2+} to form dipeptide nanoparticles, and the intrinsic fluorescence signal of the peptides shifted from the ultraviolet (UV) to the visible range due to π-π stacking interaction of aromatic groups and the structure rigidification by Zn^{2+} [63]. After being functionalized with MUC1 aptamer and Dox, the dipeptide nanoparticles could target cancer cells and image drug release in real time.

Polymeric nanovesicles obtained *via* self-assembly of amphiphilic small molecules hold a significant advantage in the ability to obtain a wide range of desired functions *via* the incorporation of hydrophobic/hydrophilic components with rational selection. A glycol nanovesicle (Lac-SS-DCM) is self-assembled by a rationally designed amphiphilic lactose derivative [59], in which a DCM moiety (used as the hydrophobic part and the fluorescence off-on probe) was pre-quenched and conjugated with a lactose derivative (used as the hydrophilic part and the targeting ligand to galectin-overexpressing tumor cells *via* enhanced carbohydrate-protein interactions) *via* a disulfide linkage (the GSH-responsive unit) (Figure 2B). The targeting Lac-SS-DCM nanovesicles were disassembled by GSH, and simultaneously activated the dormant

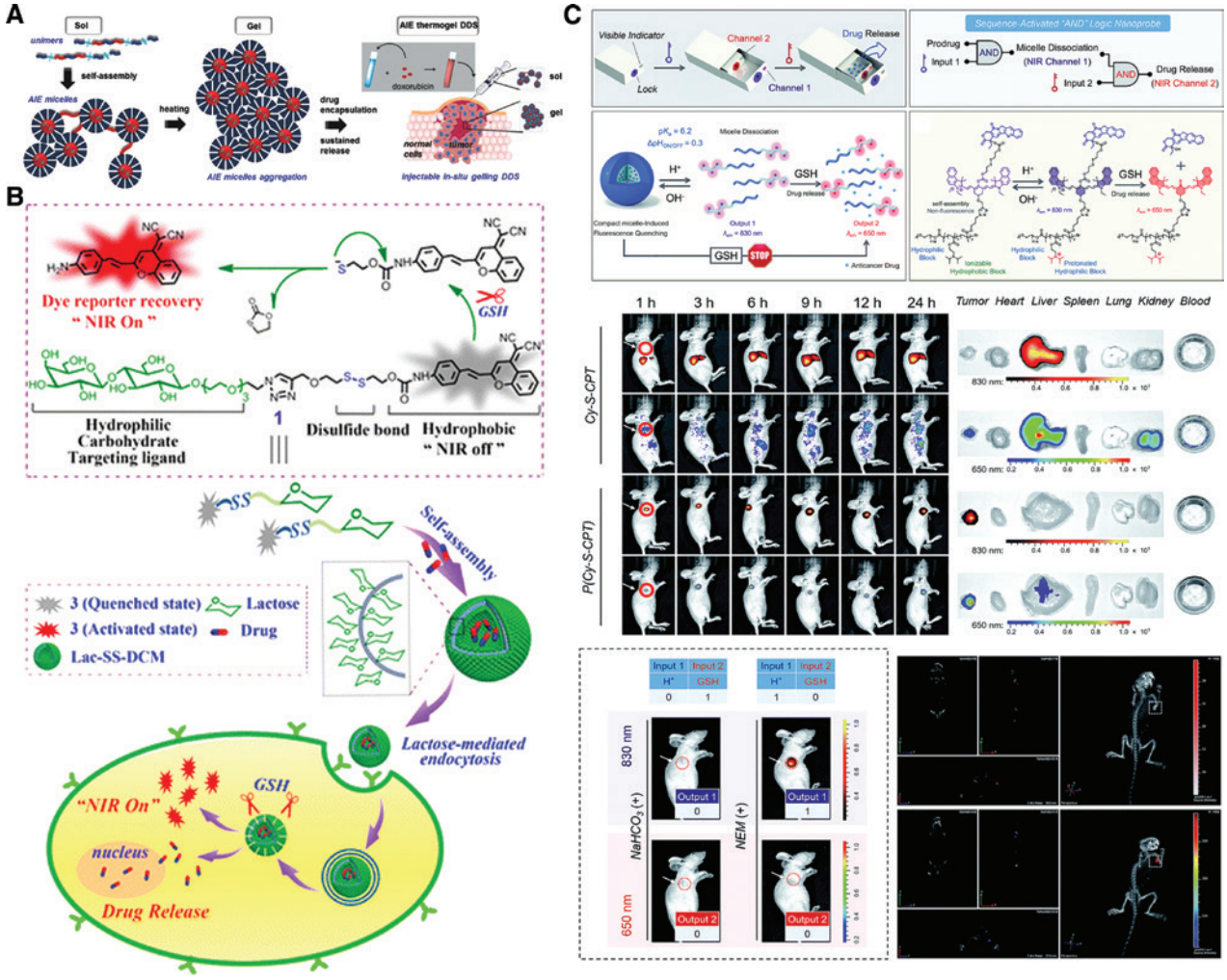

Figure 2: Monitoring drug release by fluorescent macromolecules.
(A) Schematic drawing of AIE micelles, micelle aggregation, and *in situ* gelling DDS. (Adapted from Ref. [58].) (B) Schematic illustration of assembly, lactose-mediated endocytosis, NIR fluorescence on, and drug release of Lac-SS-DCM. (Adapted from Ref. [59].) (C) Sequence-activated AND logic dual-channel NIR fluorescent probe. Also, dual-channel fluorescence tracking of the programmable drug release *in vivo* (yellow-red represented at 830 nm; rainbow represented at 650 nm). (Adapted from Ref. [60].)

NIR fluorescence of DCM, allowing the drug release triggered by the high GSH concentration in cancer cells and real-time monitoring of the release process.

For precisely controlling the drug release *in vivo*, DDSs with programmable release behaviors have been reported, which respond to multiple stimuli. Yan et al. [60] incorporated sequence-activated fluorescence responses into DDS to monitor multi-stimuli-triggered programmable drug release (Figure 2C). The smart AND logic dual-channel NIR fluorescent probe P(Cy-S-CPT) had a hierarchical structure composed of an ionizable tertiary amine-containing diblock co-polymer for rendering an ultrasensitive response to pH changes and a dual-channel NIR fluorescence component Cy-S-CPT for tracking the biothiol-triggered drug release. The programmable drug release of this hierarchical probe was conducted in a multi-stage tumor microenvironment, acidic endocytic organelles followed by abnormal GSH-overexpressing cell cytosol, which was synchronous with dual-channel NIR fluorescence output (830 and 650 nm, respectively). Impressively, *in vivo* fluorescence and 3D imaging demonstrated that P(Cy-S-CPT) could precisely target tumor tissue and perform controllable programmable drug release.

2.3 Mesoporous silica nanoparticle (MSN)-based drug release monitoring

To date, MSNs have become attractive delivery vehicles because of their unique structural features that enable high drug loading, ease in structure control, and versatility in functionalization. The ordered pore network within

these MSNs allows drug entrapping by diffusion. Meanwhile, the pores can be gated with various valves such as molecular motifs [64], nanoparticles [65–69], polymer multi-layers [70], DNA [71, 72], and proteins [73], which were designed to trigger the release of the entrapped drugs in the presence of multifarious external or internal stimuli. In light of numerous reports on the design and development of MSN-based stimuli-responsive DDSs, the development of strategies for real-time monitoring of drug release from MSNs is desired. Typically, optical agents were modified on the surfaces of MSNs or doped in the skeleton to track drug delivery and release in cells or tissues.

Lai et al. [64] designed a delicate molecular valve for the pores of MSN to control and monitor redox-responsive drug release (Figure 3A). The system comprised four components: (i) coumarin (FRET donor)-labeled-cysteine tethered MSNs as the drug carrier, (ii) fluorescein isothiocyanate (FITC, FRET acceptor)-attached β-cyclodextrin (β-CD) as the molecular cap to block the pores, (iii) disulfide linkage as the redox-responsive trigger to release the entrapped drug molecules, and (iv) FRET donor-acceptor for monitoring drug release in real time. Specifically, owing to linkage by the intact disulfide bond, the close proximity between coumarin and FITC resulted in FRET. In the presence of redox stimuli like GSH, the disulfide bond was cleaved, which led to the removal of the molecular cap (FITC-β-CD), thus triggering drug release and eliminating FRET. The release of the drugs from the MSN nanocarrier was monitored in real time following the changes in the FRET signal. It was also demonstrated that any exogenous or endogenous change in the GSH concentration would result in a change in the amount of released drug as well

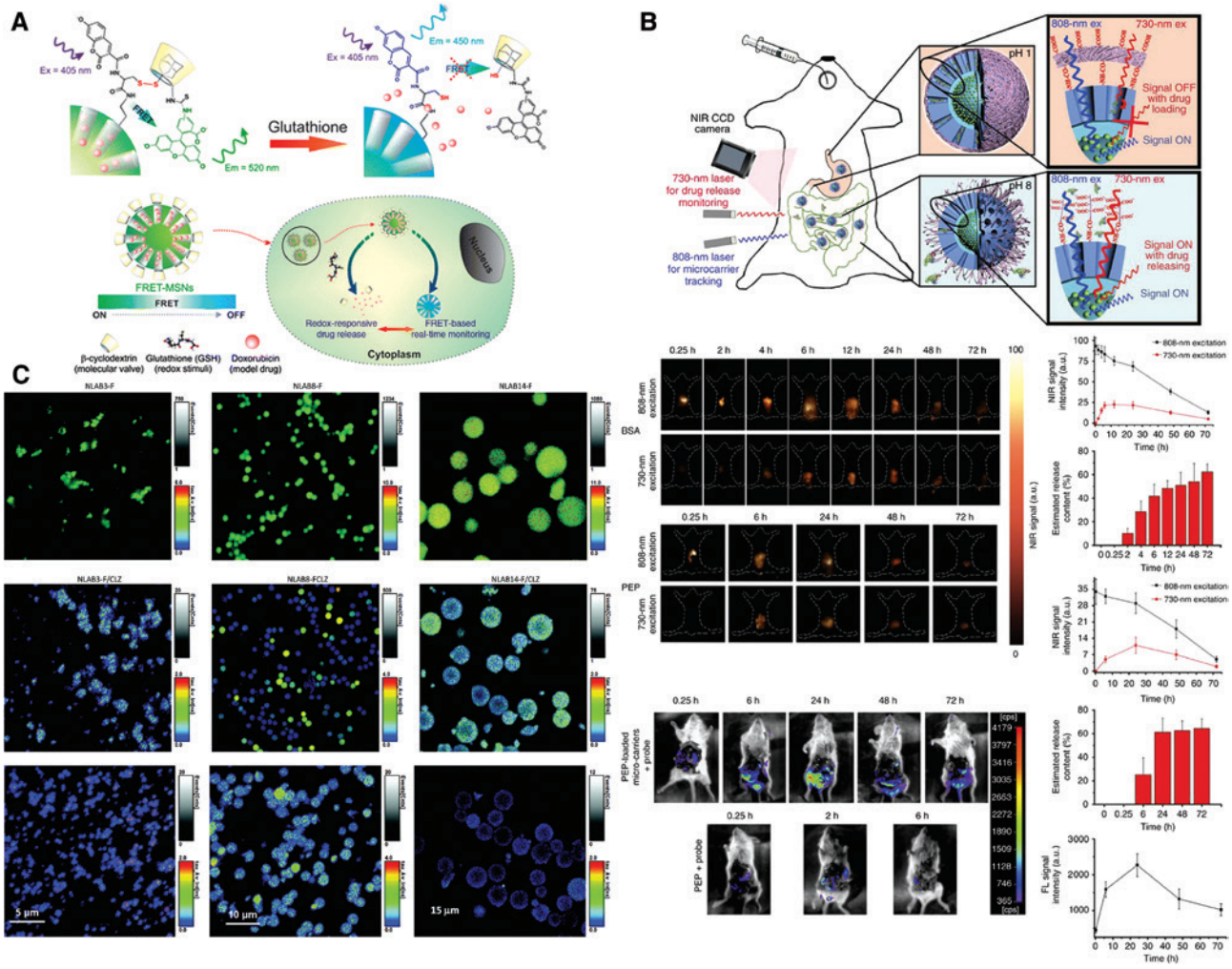

Figure 3: Monitoring drug release by fluorescent MSNs.
(A) Schematic representation of the redox-responsive FRET-MSNs. (Adapted from Ref. [64].) (B) Microcarrier fate tracking and drug release monitoring in the NIR-II window using an InGaAs charge coupled device (CCD) camera. (Adapted from Ref. [74].) (C) Fluorescence lifetime imaging for drug release monitoring. (Adapted from Ref. [75].)

as concurrent change in the FRET signal, suggesting that the FRET-based MSNs could be applied to monitor the release of different drugs in real time.

By using SiO_2 as template, Chen et al. [76] synthesized rare-earth (Tb, Eu)-doped Gd_2O_2S-based radioluminescent capsules with an X-ray-excited optical luminescence that changed during the release of the absorbing chemotherapy drug, Dox. *In vitro* experiments have demonstrated the pH-triggered release process of Dox from nanocapsules coated with a pH-responsive polyelectrolyte multi-layer. The Dox was loaded over 5% by weight and released from the capsule with a time constant of ~36 days at pH 7.4 and 21 h at pH 5.0, respectively. Other nanomaterials with specific functions are also combined with mesoporous silica to precisely control drug release. For example, metallic nanoparticles, such as gold and silver nanoparticles, have been widely explored for application in cancer diagnosis and therapies due to their fascinating properties. Gold nanorods (AuNRs) exhibit strong absorption and photothermal effect in the NIR region owing to their longitudinal localized surface plasmon resonance. Lee et al. [77] developed a NIR-responsive DDS based on mesoporous silica-coated AuNRs (AuNR@$mSiO_2$) and phase change material (PCM). The AuNR core in AuNR@$mSiO_2$ provided excellent NIR sensitivity and could efficiently quench the fluorescence of Dox, while the mesoporous silica shell provided an increased reservoir of the loaded drug (Dox). The PCM was applied as both a thermosensitive gatekeeper and a medium for loading hydrophobic anti-cancer drugs. The photothermal effect of the AuNRs under NIR irradiation could heat the PCM above its phase transition temperature and facilitate a rapid release of Dox and concurrently fluorescence recovery. An enhanced anti-cancer effect was observed against various cell lines, and the intracellular release of the drug was easily monitored by live cell imaging.

Shan et al. [78] covalently modified the mesoporous channel with the ligand thenoyltrifluoroacetone firstly to *in situ* immobilize Yb^{3+} ions, thus forming a Yb(III) complex. Then, the two-photon ligand 4,4′-bis[p-(diethylamino)-α-styryl]-2,2′-bipyridine was used to coordinate with the central Yb^{3+} ions to make the Yb(III) complex possess the NIR excitation (850 nm) and NIR emission (980 nm) property. Dox was then embedded into the mesoporous silica channel by coordination and π-π interaction with the Yb(III) complex, resulting in the decrease of photoluminescence intensity of the Yb(III) complex. Upon the drug release, the photoluminescence intensity of the Yb(III) complex became stronger because the coordinated Dox diffused out and the coordination sphere of the central Yb^{3+} ions changed, thus achieving real-time drug release monitoring.

Compared to fluorescence imaging in visible range (400–750 nm) and the first NIR (NIR-I) window (750–900 nm) with low tissue penetration depth of several micrometers to millimeters because of severe absorption and scattering of photons by tissues, the second NIR (NIR-II) window (1000–1400 nm) features deeper penetration depths (1–2 cm) and higher resolution (sub-10 μm) with reduced scattering and minimized autofluorescence. Wang et al. [74] reported a novel microcarrier by integrating lanthanide-based nanoparticles ($NaGdF_4$: 5%Nd@$NaGdF_4$) emitting in the NIR-II window with MSNs (Figure 3B). The microcarrier realized *in vivo* semi-quantitative detection of the released drug in real time by measuring the fluorescence signals in the NIR-II window of lanthanide-based nanoparticles with an absorption competition-induced emission bioimaging system. The authors demonstrated that the microcarriers showed a prolonged residence time in the gastrointestinal tract up to 72 h and released up to 62% of the loaded drug. Moreover, minimal deposition of the microcarriers was found in non-target organs, such as the liver, spleen, and kidney. These findings provide novel insights for the development of therapeutic and bioimaging strategies.

Except for the fluorescence imaging relying on the intensity or spectral shift, fluorescence lifetime imaging is also a very attractive imaging tool for biomedical application, because it can reflect instantaneous local changes and allow distinguishing them from autofluorescence of the biological environment [79–81]. In view of these appealing features of fluorescence lifetime imaging, Valetti et al. [75] prepared label-free fluorescent mesoporous silica micro- and nanoparticles through *in situ* generation of carbon dots within the pores. By controlling the thermal decomposition of carboamino groups linked on the surface, three different types of mesoporous silica particles were synthesized: NLAB3, NLAB8, and NLAB14. The particles were endowed with emission in the visible region and had fluorescence lifetimes of up to 9.0 ns, which could be easily discriminated from intrinsic biological autofluorescence. The drug release was monitored successfully in biological environments by means of fluorescence lifetime imaging (Figure 3C).

2.4 Quantum dot (QD)-based drug release monitoring

QDs with the size of few nanometers are appealing candidates for nanodelivery and as optical probes in biomedical applications due to their excellent photostability, metabolic stability, and photoluminescence. Recently, several QDs such as carbon dots and silicon dots have been used

to monitor drug release. Usually, the QDs were embedded into or capped onto nanocarriers to track the DDS and monitor drug release.

Carbon nanodots (CDots), owing to their high photostability, good water solubility, excellent biocompatibility, and multi-photon absorption, have emerged as a new class of fluorescence probes [82] and have also been extensively investigated for numerous applications, such as in medical imaging, in disease diagnosis, and as a print ink [83–85]. Tang et al. [86] reported a FRET-based CDot DDS (FRET-CDots) *via* directly coupling PEG onto the CDot surface followed by trapping the guest drug molecules within the PEG network and attaching to the CDot surface by π-π stacking, enabling real-time monitoring of drug release on the basis of the FRET signal (Figure 4A). In this case, the close proximity between CDots (serving as both excellent drug carriers and the donors) and Dox (the acceptor) made them form a FRET pair (FRET on). When the CDots were excited at 405 nm, emissions of both 498 and 595 nm were displayed, which correlated with the intrinsic emission of CDots and energy transfer from CDots to Dox, respectively. When Dox molecules are released from the CDot surface in the acidic environment, the FRET between CDots and Dox is terminated (FRET off), thus displaying an enhanced emission at 498 nm. This change in FRET signal could easily be regulated by the release of drug molecules from the CDot surface, thus allowing for convenient cell imaging and direct monitoring of the drug release process in real time. Moreover, the 3D two-photon imaging of the FRET-CDot at tumor tissues of 65–300 μm under the excitation of 810 nm suggested that the CDots had the potential to monitor drug release in deep tumor tissues.

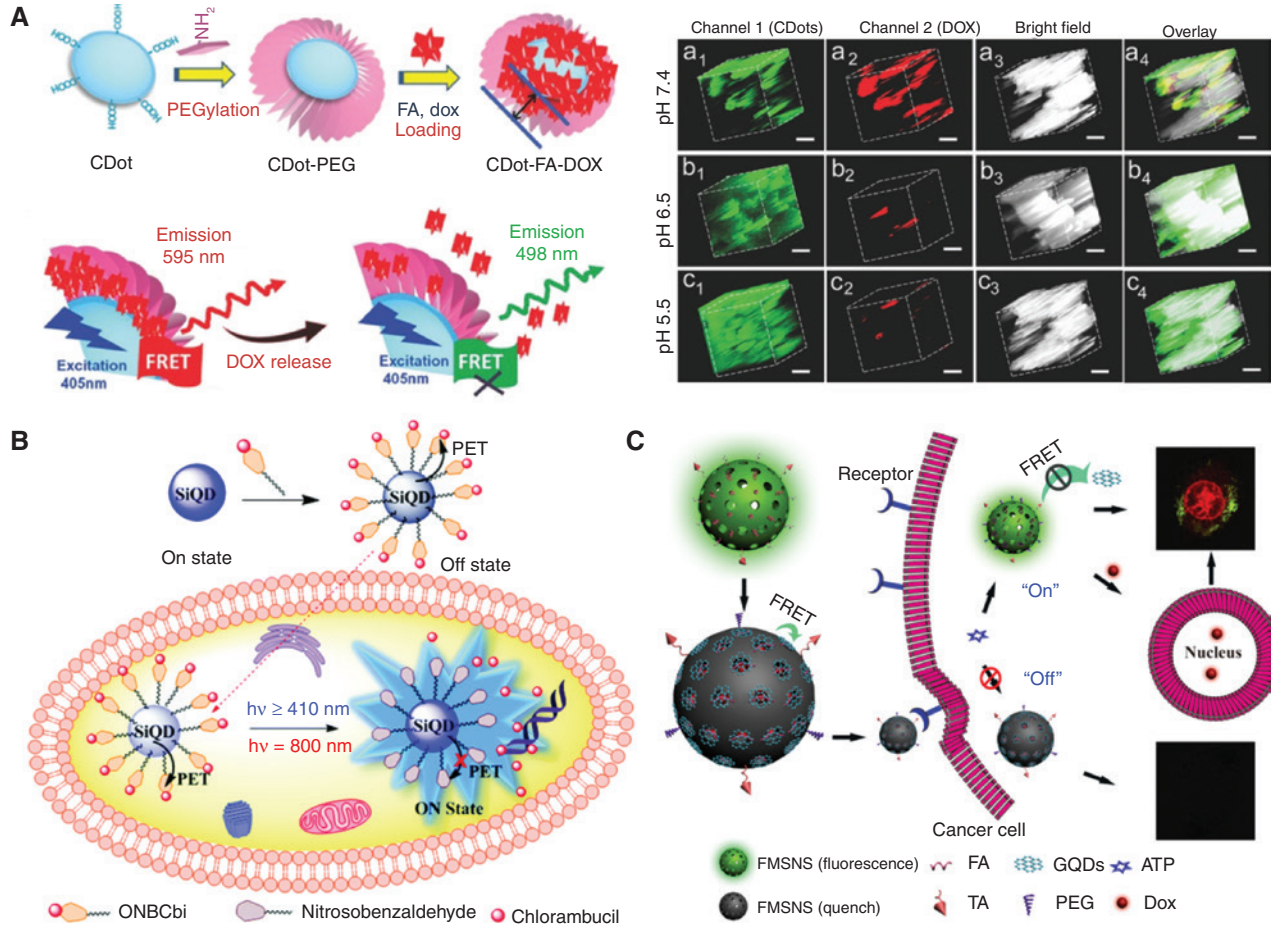

Figure 4: Monitoring drug release by QDs.
(A) Schematic representation of the FRET-CDot-DDS for drug delivery. Also, 3D two-photon confocal fluorescence images (under 810-nm excitation) of CDot-FA-Dox conjugate-incubated glomerular tissues, accumulated along the z-direction at a depth of 65–300 μm, incubated under pH of a) 7.4, b) 6.5, and c) 5.5. (Adapted from Ref. [86].) (B) Schematic representation of controlled release and real-time monitoring of the anticancer drug chlorambucil from ONBCbl-SiQDs. (Adapted from Ref. [87].) (C) Preparation and application of ATP-responsive GQDs-based nanocarriers. (Adapted from Ref. [88].)

Photoluminescent silicon QDs (SiQDs) have great potential in the area of fluorescence imaging owing to their unique properties, such as tunable emission, high natural abundance, low toxicity, and excellent surface tailorability [89], driving them be well explored as *in vitro* [90–92] and *in vivo* [93, 94] imaging agents. Recently, SiQD-based DDSs, which are responsive to pH changes, have been reported [95–97]. Paul et al. [87] used SiQDs as biocompatible fluorescent nanocarriers and o-nitrobenzyl (ONB) derivative as a phototrigger to construct a photoresponsive SiQD-based DDS (ONBCbl-SiQDs) for the controlled release of the anti-cancer drug chlorambucil (Figure 4B). The ONB moiety with the caged anti-cancer drug chlorambucil quenched the fluorescence of SiQDs due to the photoinduced electron transfer process, which was termed as the fluorescence "off" state. Upon irradiation with one photon or two photons, uncaging of the drug occurred and led to the fluorescence recovery of SiQDs, considered as the fluorescence "on" state. This photoswitchable fluorescence signal was used to monitor drug release in real time.

Luminescent gold nanoclusters (AuNCs) consisting of several to tens of gold atoms have recently attracted significant scientific interest in fluorescence imaging. Importantly, the latest research showed that aggregated thiolate-AuNCs exhibited enhanced luminescence owing to the mechanism of AIE, and this phenomenon was closely connected to the restriction of intramolecular motion. Cao et al. [98] encapsulated aggregated AuNCs (aAuNCs) into metal-organic frameworks (MOFs, ZIF-8), which restricted the free movements of AuNCs in aggregated states, and thus enhanced their luminescence with an improved quantum yield of up to 7.74%. Once the acidic pH-induced dissociation of the ZIF-8 framework occurred, the aAuNCs were liberated from the MOF and dispersed in the form of individual nanoclusters with weaker luminescence. By encapsulating the hydrophobic drugs into the luminescent MOF simultaneously, the aAuNC-MOFs can achieve controlled release under acidic conditions and real-time imaging of pH-dependent drug release.

Graphene QDs (GQDs) maintaining the intrinsic layered structural motif of graphene have emerged as promising nanomaterials for fluorescence imaging and biosensing [99–102] due to their small lateral size, fine optical property, and superior biocompatibility. Our group has fabricated a smart drug nanocarrier based on FRET by capping GQDs (the acceptor) onto fluorescent MSNs (the donor) *via* ATP aptamer for real-time monitoring of ATP-triggered drug release [88] (Figure 4C). In this work, GQDs were used as both gatekeeper and quencher. By virtue of the sensitive interaction between ATP and ATP aptamer, any exogenous or endogenous fluctuation in the ATP concentration resulted in a change in drug release and concurrent variation in the FRET signal, which allowed real-time monitoring the release of drug from the pores.

2.5 Upconverting nanoparticle (UCNP)-based ratiometric luminescence for drug release monitoring

UCNPs are promising for bioimaging and biosensing owing to their minimized photodamage, suppressed autofluorescence, and high tissue penetration depth [103–108]. The unique ability of upconverting low-energy NIR light to high-energy UV, visible, and NIR light makes UCNP an excellent nanotransducer for controlled drug release and an outstanding tracer for monitoring the drug release.

Wang et al. [109] coated a mesoporous SiO_2/Ca layer onto UCNP to form UCNPs@mSiO_2-Ca core-shell nanocomposites, which were able to deliver anti-cancer drugs and monitor drug release. Generally, the $NaYF_4$:Yb/Er UCNPs exhibited strong green emission (around 550 nm) and weak dark red emission (around 660 nm). Here, the incorporation of Ca into the nanocomposites induced phase transformation from a pure hexagonal phase to a cubic phase, and facilitated the occurrence of red emission, which strongly overlapped with the maximum absorbance of the anti-cancer drug zinc phthalocyanine to form a FRET pair. Consequently, drug release could be quantified by monitoring the luminescence recovery of UCNPs.

The simultaneous multiplex emission of UCNP in the UV to NIR range is important for the design of multifunctional UCNP-based DDS: (i) the individual sharp emission peaks in the UV-visible region can serve as an energy donor for luminescence resonance energy transfer (LRET) to the entrapped drugs that typically absorb in UV-visible range, thereby allowing for real-time monitoring of the release of different drugs, whereas (ii) the NIR emission remains constant irrespective of the drug molecule and hence can be used for imaging or quantifying the drug release *via* a ratiometric signal. The conventional method to monitor the drug release using a single signal may be affected by an unknown local concentration of nanocarriers and uncontrolled microenvironment change in biological samples. Li et al. [110] presented a rational design for ratiometric monitoring of drug release kinetics in living cells by virtue of the multi-color emission feature of UCNPs (Figure 5A). In the system of mesoporous silica-coated $NaYF_4$:Yb,Er nanocomposites loaded with Dox ($NaYF_4$:Yb,Er@mSiO_2-Dox), the green upconversion

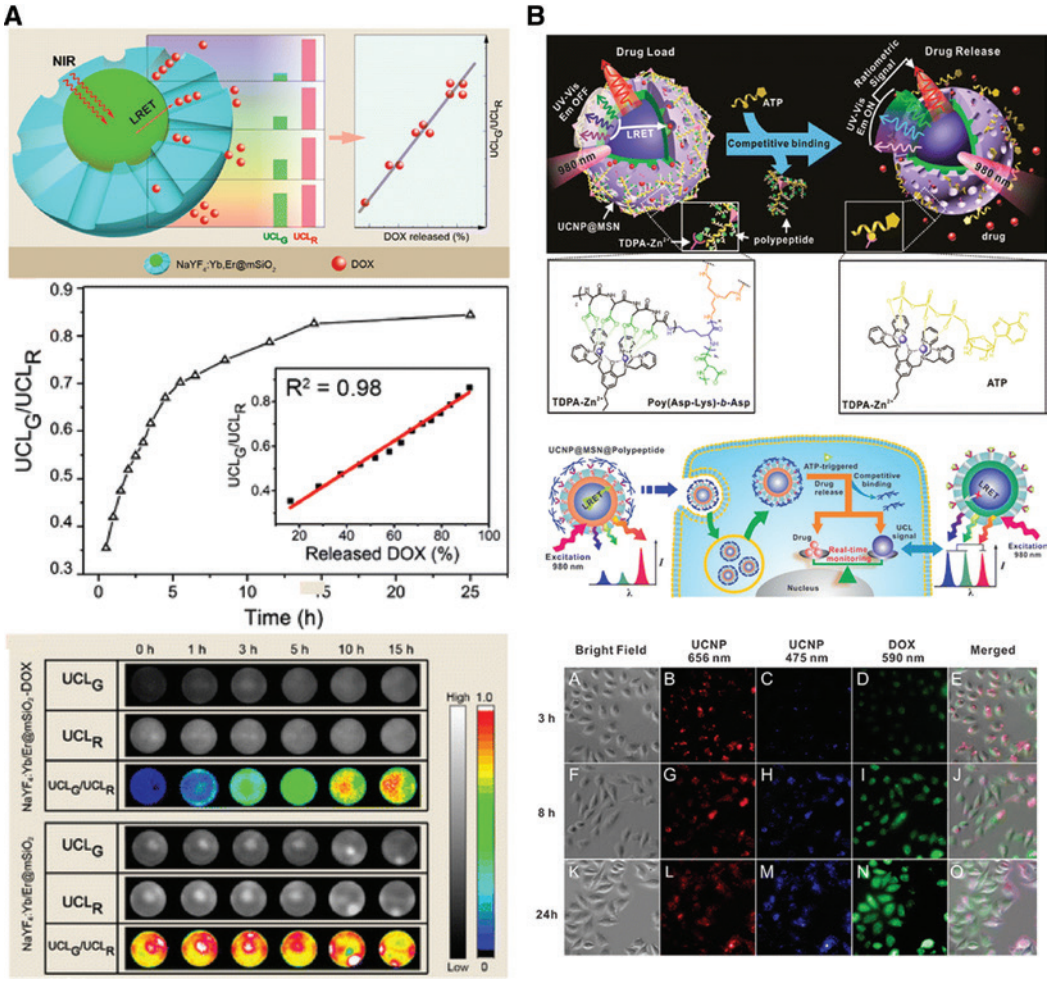

Figure 5: Ratiometric monitoring of drug release by UCNPs.
(A) Schematic illustration of LRET-based upconversion nanocarriers for Dox delivery and the linear relationship between the Dox release percentage and UCL_G/UCL_R ratio. UCL_G and UCL_R denote green and red upconversion luminescence, respectively. (Adapted from Ref. [110].)
(B) Schematic representation of the real-time monitoring of ATP-responsive drug release from polypeptide-wrapped TDPA-Zn^{2+}-UCNP@MSNs. Also, the intracellular drug release was monitored by UCL imaging. (Adapted from Ref. [111].)

luminescence (UCL_G) of the $NaYF_4$:Yb,Er nanoparticles was selectively transferred to the drug Dox through the LRET mechanism, while the red upconversion luminescence (UCL_R) was essentially unchanged and used as an internal standard. This ratiometric design employed red emission as the internal standard, and thus offered an accurate and reliable platform for localized drug delivery monitoring in living cells, avoiding the interference of the internal microenvironment and dosing errors. A linear relationship between the green-to-red emission intensity ratio (UCL_G/UCL_R) and the percentage of the released Dox was established.

Almost simultaneously, Lai et al. [111] utilized the multi-color UCNP with a core-shell structure of β-$NaYF_4$:Yb^{3+}/Tm^{3+}@$NaYF_4$:Yb^{3+}/Er^{3+} to construct a ratiometric probe for monitoring drug release (Figure 5B). Such a core-shell structure of UCNP minimized the cross relaxation of activators, endowing the UCNP with bright emissions in the UV to NIR region (360, 475, 542, and 656 nm) when excited with a 980-nm NIR laser. This multi-color upconversion nanoparticle was firstly coated by mesoporous silica to form a UCNP@MSN composite nanoparticle. After being functionalized with zinc dipicolylamine analogue (TDPA-Zn^{2+}), a compact branched polypeptide, poly(Asp-Lys)-b-Asp, was wrapped on its exterior surface through multi-valent interactions to entrap the drugs in interior mesopores. The UCNP emission in the UV-visible range was quenched due to LRET from the UCNPs to the entrapped drugs, while retaining their strong NIR emission. ATP had higher affinity to TDPA-Zn^{2+} and competitively displaced the surface bound polypeptide, which led to the release of the entrapped drugs and subsequent collapse of LRET. The intracellular drug release was accompanied with the enhancement in the UV-visible

emission of UCNP, which allowed for real-time monitoring of the drug release *via* a ratiometric signal with the NIR emission of UCNP as an internal reference.

3 MRI for drug release monitoring

MRI is based on the spin-lattice relaxation (T_1 contrast) or the spin-spin relaxation (T_2 contrast) times of protons contained in different microstructures of the organs to create imaging contrast. As a powerful imaging modality in clinical medicine, MRI is a promising candidate for monitoring the biodistribution and site-specific accumulation of DDSs because it can produce non-invasive, tissue-depth-independent images with high spatial and temporal resolutions [112–114]. To improve its imaging sensitivity and resolution, paramagnetic ions, such as gadolinium (Gd^{III}) [115, 116], manganese (Mn^{II}) [117], and iron (Fe^{III}) [118], are typically used as MRI contrast agents to provide magnetic functionality. These ions can be intrinsic to the nanoparticles, incorporated as a dopant within a non-magnetic matrix, or attached to the surface of a nanoparticle *via* chelation [119]. Moreover, MRI is exquisitely suitable for monitoring drug release and drug efficacy. Because MRI contrast agents depend on access to freely diffusing water molecules to generate contrast, and therefore render different signals when drug molecules present within vs. outside of a nanocarrier, they provide optimal conditions for assessing drug release [120]. Recently, various nanoparticle-based contrast agents were developed to monitor drug release using MRI by right of the interaction between drug molecules and the MRI contrast agent. In particular, stimuli-responsive MRI nanosystems have been constructed typically in which magnetic resonance (MR) signals were turned off by forming complexes or encapsulated with drugs to shield the paramagnetic ions from the surrounding water. After triggering by endogenous or exogenous stimuli, such as pH, small molecules, temperature, or light, the MR signals show detectable changes along with the liberation or exposure of paramagnetic ions. These unique properties make MRI potentially applicable for drug release monitoring.

3.1 Gd-based MRI agents for drug release monitoring

As commercial MRI contrast agents, gadolinium chelates that can produce positive contrast enhancement in T_1-weighted MRI are beneficial for tumor diagnosis. Our group reported intelligent biodegradable DDS-based gadolinium-Dox-loaded nanoscale coordination polymers (Gd NCPs) for targeted drug delivery and programmed drug release [121]. As shown in Figure 6A, the gadolinium ions not only acted as metallic nodes to conjugate the building blocks of 2-amino-1,4-benzenedicarboxylic acids (NH_2-BDC) to form uniform nanoparticles, but also as anchors to chelate Dox to form Gd^{3+}-Dox complexes. Meanwhile, the gadolinium atoms in the core of the Gd NCPs were shielded well from water, making no contribution to T_1-weighted MRI contrast. By further coating a hyaluronic acid shell, the designed multi-functional nanocarriers were taken up especially by CD44-positive cancer cells *via* receptor-mediated endocytosis, and trapped within the lysosomes and endosomes. The acidic environment of lysosomes and endosomes caused the decomposition of the Gd NCPs into small fragments, along with the release of Dox. Therefore, water molecules could access the gadolinium atoms, manifesting as a "turned-on" T_1 signal for drug release monitoring. *In vitro* experiments showed that the Gd NCPs exhibited enhanced T_1 signal under acidic condition, suggesting their potential for localizing the tumor and monitoring drug release.

Kaittanis et al. [123] constructed a polymeric nanobeacon by chelating glucose-based polymer dextran with 89-zirconium and gadolinium. The positron emitter 89-zirconium could not merely image the tumor by positron emission tomography, but also guide the surgical resection of sentinel lymph nodes by their inherent Cerenkov luminescence. The MRI contrast agent gadolinium allowed monitoring the drug release with MRI through the quenching of the gadolinium signal by the co-loaded drug. Kim et al. [124] developed short-chain elastin-like polypeptide-incorporating thermosensitive liposomes (STLs) to co-encapsulate gadobenate dimeglumine (Gd-BOPTA) and Dox (Gd-Dox-STL). Gd-Dox-STL was highly stable under physiological conditions (37°C) and capable of rapidly releasing the encapsulated drug with mild hyperthermia (42°C) induced by high-intensity focused ultrasound (HIFU). Compared with lysolipid-based temperature-sensitive liposome loaded with gadolinium-based MRI contrast agent and Dox (Gd-Dox-LTSL), the Gd-Dox-STLs have higher stability and larger changes in T_1 relaxation time between 37°C and 42°C. *In vivo* MRI experiments demonstrated the co-release of Dox and Gd-BOPTA from STL under HIFU-induced mild hyperthermia, and thus the effectiveness of drug delivery and heating-triggered drug release could be assessed by detecting the MRI signals.

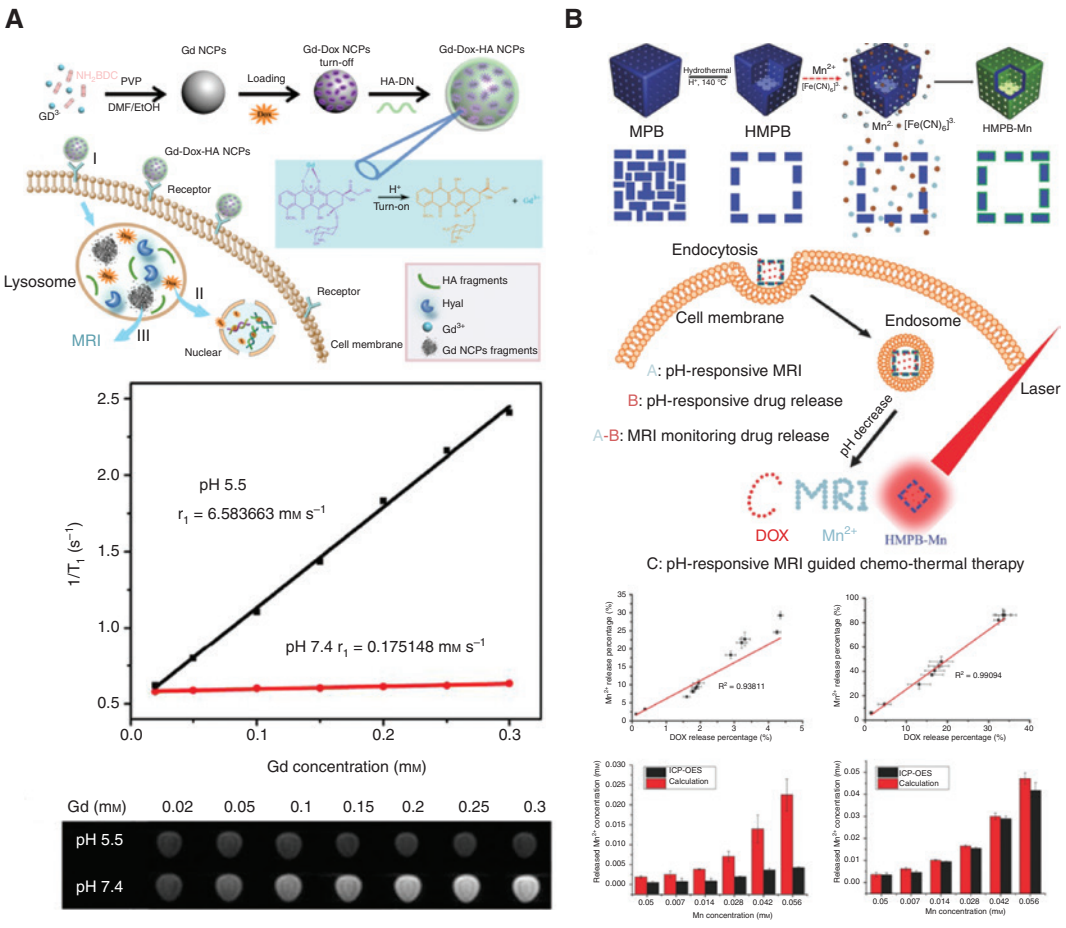

Figure 6: Monitoring drug release by Gd/Mn based MRI contrast agents.
(A) Schematic illustration of an acid-degradable gadolinium-based nanoscale coordination polymer. r_1 relaxivity curves and T_1-weighted MR images of Gd NCPs with various Gd^{3+} concentrations at pH 5.5 and 7.4, respectively. (Adapted from Ref. [121].) (B) Schematic illustration of the synthetic procedure of HMPB-Mn, and schematic representation of HMPB-Mn as a smart multifunctional theranostic for pH-triggered T_1-weighted MRI monitoring of drug release and tumor chemothermal therapy. The correlation between Dox release and Mn^{2+} release of HMPB-Mn at pH 7.4 and pH 5.0; comparison of the calculated Mn^{2+} concentrations by MRI intensity measurement and the release Mn^{2+} concentrations measured by inductively coupled plasma optical emission spectrometry (ICP-OES) at pH 7.4 and pH 5.0. (Adapted from Ref. [122].)

3.2 Mn-based MRI agent for drug release monitoring

The Mn-based agent is one kind of the earliest reported examples that can be used for enhancing T_1-weighted MRI owing to its efficient positive contrast enhancement. Cai et al. [122] constructed a smart Prussian blue-based theranostic nanoplatform with a core-shell hollow structure (namely HMPB-Mn) by coating an Mn-containing Prussian blue analogue (MnPBA) onto the outer surface and the inner channels of hollow mesoporous Prussian blue nanoparticles (HMPBs) (Figure 6B). The HMPB-Mn was highly sensitive to acidic pH and could release Mn^{2+} at the tumor site, making HMPB-Mn a smart T_1-weighted MRI contrast agent with ultrahigh relaxivity for tumor diagnosis. Meanwhile, the hollow mesoporous structure and high surface area endowed HMPB-Mn with high drug (Dox) loading capacity for tumor chemotherapy. More important, both Mn^{2+} ions and Dox molecules were released concurrently from the prepared HMPB-Mn in a pH-triggering manner, and the Dox release rate was real-time monitored through MRI. Combining the high-efficiency chemotherapy and excellent photothermal conversion property, HMPB-Mn also showed a great potential in synergistic chemothermal therapy.

Dong et al. [125] doped Mn^{2+}-chelated chlorine e6 [Ce6(Mn), a photosensitizer for photodynamic therapy] into mono-dispersed PEG-modified mesoporous $CaCO_3$ nanoparticles by co-precipitation. The as-synthesized mesoporous structure of Ce6(Mn)@$CaCO_3$-PEG nanoparticles could enable efficient loading of chemotherapeutic agent, Dox. With the degradation of the

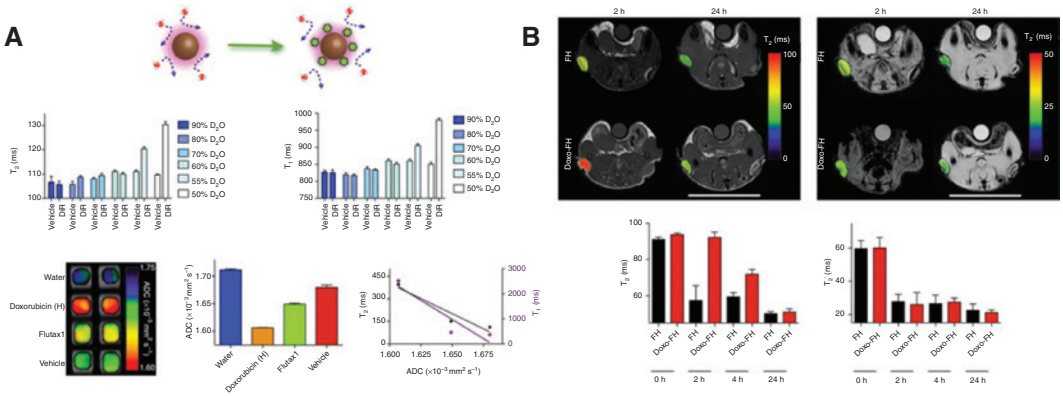

Figure 7: Monitoring drug release by Fe based MRI contrast agents.
(A) Schematic representation of the proposed model suggesting that the presence of cargo within the coating of iron oxide nanoparticles hinders the diffusion of water molecules, concomitantly affecting the ability of nanoparticles to efficiently diphase the protons of water. (B) Non-invasive monitoring of drug release *in vivo* with MRI. (Adapted from Ref. [126].)

nanoparticles under weak acidic solutions, Ce6(Mn) and Dox were released attendant with the significantly enhanced T_1-contrast under MRI, making it possible to monitor the pH-dependent drug release in real time. Additionally, as guided by MRI and fluorescence imaging, it was found that the intravenously injected $CaCO_3$@Ce6(Mn)/Dox-PEG could gradually accumulate in the tumor and contribute to a synergistic anti-tumor effect in the combination of photodynamic therapy and chemotherapy.

3.3 Fe-based MRI agent for drug release monitoring

Although iron oxide nanoparticles as T_2 contrast agents have been widely used in MRI, they are rarely applied for drug release monitoring. Kaittanis et al. [126] reported that the clinical formulation of polymer-coated iron oxide nanoparticles (ferumoxytol) could serve as a DDS in cancer chemotherapy (Figure 7). Specifically, the dextran coating retained diverse therapeutic payloads *via* weak electrostatic interactions. Once perturbed by mild acidification, the particles could rapidly release their cargo, which was utilized for the treatment of solid tumors. In addition to the improved therapy efficacy, the spatiotemporal drug release was monitored *via* MRI as the cargo release restored the spin-spin (T_2) and spin-lattice (T_1) relaxation signals of ferumoxytol, while leaving the T_2^* signature unchanged. In such a self-reporting multi-functional drug delivery platform, neither the particle nor the drug is subject to any chemical modification, which could lead to a faster administrative approval.

4 SERS imaging for drug release monitoring

SERS is an optical phenomenon in which the Raman scattering cross section can be increased by >6 orders of magnitude when the probe molecules are deposited on a roughened metal surface, which was first observed by Fleischmann in 1974 [127]. Since then, SERS has been widely used for biological sensing or molecular imaging as an ultrasensitive spectroscopic tool for interface studies [128]. The SERS method offers several advantages [129–132], including (i) ease of sample preparation, (ii) availability of characteristic peaks for label-free "fingerprinting," (iii) narrow peak width for multiplexing detection, and (iv) good stability against photobleaching. Recently, Raman microscopy has made great progress in monitoring drug release. Some drug molecules such as thiopurine or mitoxantrone showed enhanced Raman scattering signal with the aid of gold nanostructures, which depends on the distance between the drug molecules and the nanoparticle surface. Therefore, the drug release process can be evaluated using the Raman signals of drug molecules, providing a promising method to monitor drug release in real time.

Thiopurine anti-cancer drugs can be adsorbed on the gold nanoparticle (Au NP) surface through its N and S atoms. Ock et al. [133] investigated GSH-induced drug release on Au NP surfaces by means of label-free confocal Raman spectroscopy (Figure 8A). Direct monitoring of GSH-triggered release of 6-mercaptopurine (6MP) and 6-thioguanine (6TG) was achieved in real time. The live cell imaging technique provides a signal from nanomolar range release of 6MP and 6TG on Au NP surfaces after the injection of external GSH. The *in vivo* SERS spectra of 6TG

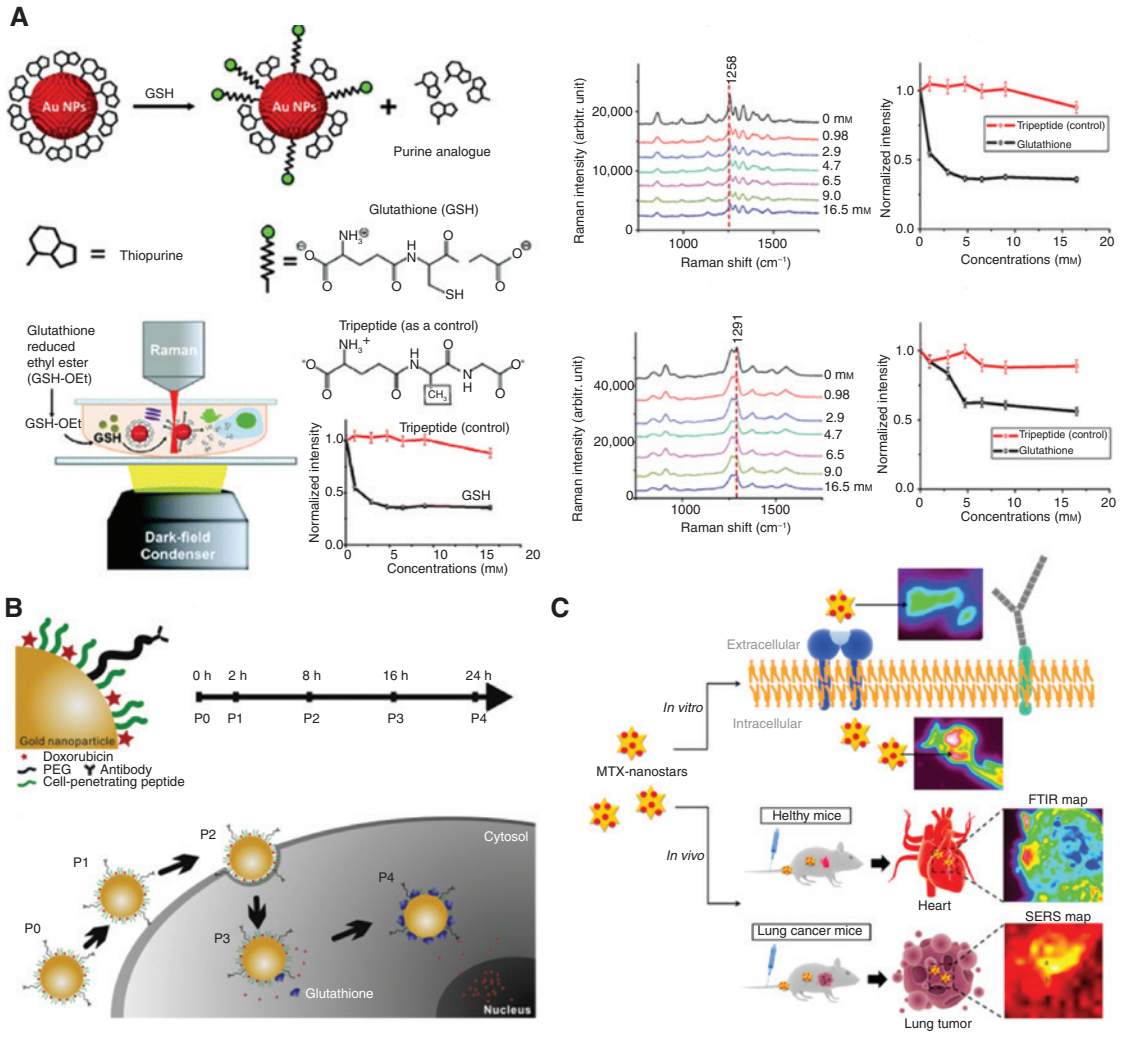

Figure 8: SERS based drug release monitoring.
(A) Experimental scheme of thiopurine release from Au NPs *via* GSH and measurements by observing a decrease in its SERS intensities in real time. The peaks at 1258 and 1291 cm^{-1} were used to compare the relative intensities from 6MP and 6TG, respectively. (Adapted from Ref. [133].) (B) Schematic diagram for conjugation of the biohybrid nanoparticle and uptake of the Dox-loaded biohybrid nanoparticles by the cells and the intracellular release of Dox by GSH. (Adapted from Ref. [134].) (C) Gold nanostars for theranostics: intracellular and *in vivo* SERS detection combined with real-time drug delivery using plasmonic-tunable Raman/FTIR imaging. (Adapted from Ref. [135].)

were obtained from the subcutaneous sites in living mice after GSH treatment. However, non-targeted therapeutic nanoparticles may cause harmful effects to healthy cells. In view of this, Hossain et al. [134] proposed an *in situ* label-free intracellular drug release monitoring system by using biohybrid nanoparticle based on SERS (Figure 8B). The biohybrid nanoparticle consisted of Au NP, cell-penetrating peptide (Tat peptide), and cancer-targeting antibody (anti-HER2 antibody) to obtain high anti-cancer efficacy with specific targeting and increased uptake rate. Both time-dependent and GSH-mediated intracellular release of Dox from the biohybrid nanoparticle was monitored with change of intracellular SERS signals of Dox. This proposed monitoring system made specific cancer cell targeting and the improved uptake of the anti-cancer drugs detectable, and the intracellular release of the anti-cancer drug visible.

Compared to Au NPs, gold nanostars with sharp-shaped metal surfaces display two surface plasmon bands consistent to the transverse and longitudinal surface plasmon bands in the visible and NIR regions, respectively. Tian et al. [135] proposed a new theranostic strategy based on efficient plasmonic-tunable Raman/Fourier transform infrared (FTIR) spectroscopy imaging to track the delivery and release of an anti-cancer drug from nanostars in living cells and its biodistribution *in vivo* (Figure 8C). Mitoxantrone was conjugated onto the surface of gold nanostars with a carboxylated PEG spacer *via* amide bonding. By

taking advantage of this system, the delivery and release of mitoxantrone from gold nanostars in single living cells and in mice were tracked in real time, revealing a strong drug accumulation in the heart of healthy mice and infiltration in the tumor tissue of lung cancer-bearing mice at 5 h after systemic injection.

5 Multi-mode imaging for drug release monitoring

Although current imaging modalities show a lot of unique advantages, each of them also has its own intrinsic limitations, such as the insufficient spatial resolution of fluorescence imaging, difficult quantitative analysis of SERS imaging, and low sensitivity of MRI. These limitations make it difficult to gather accurate and reliable information at the disease site by using just one kind of imaging modality. To address these issues, there is an increasing demand for building up a complementary multi-mode imaging and monitoring method within one system.

5.1 Fluorescence- and MRI-based multi-mode drug release monitoring system

Liu et al. [136] reported a novel concept of real-time monitoring of NIR-triggered drug release *in vitro* and *in vivo* simultaneously by using upconverted luminescence (UCL) and MRI. Such a monitoring strategy featured the characteristics of high-sensitivity of UCL as well as high resolution and tissue depth independence of MRI. Concretely, multi-functional $NaYF_4$:Yb/Tm@$NaGdF_4$ core/hollow mesoporous silica shell nanoparticles (Gd-UCNP@$hmSiO_2$) were synthesized and applied in the dual-mode imaging nanosensor. Figure 9A illustrates the prototype nanosensor containing three essential components: (i) modified "photomechanical" azobenzene that acted as a "stirrer" on the mesopore surface of Gd-UCNP@$hmSiO_2$

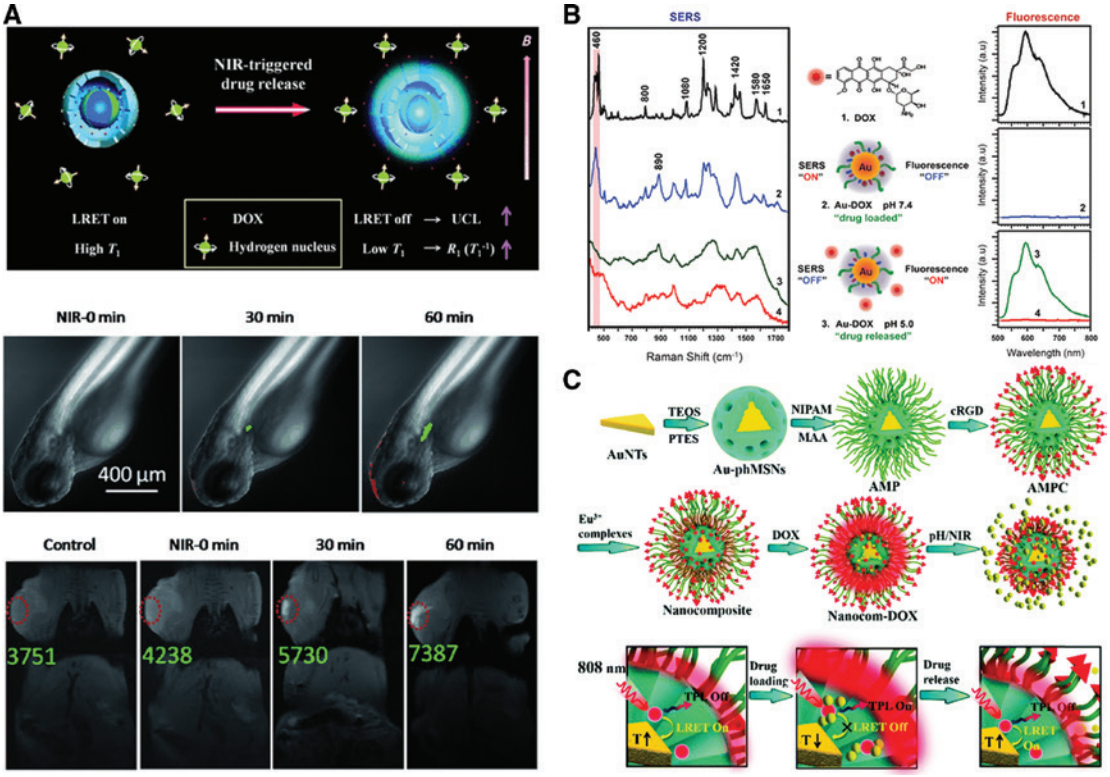

Figure 9: Multi-mode imaging for drug release monitoring.
(A) UCL/T_1-MRI dual-mode nanosensor for drug release monitoring: confocal laser scanning microscopy images of zebrafish, in which UCNP signals are green and Dox signals are red; T_1-MR images of a Walker-256 tumor-bearing Sprague-Dawley rat injected with nanosensor subcutaneously before and after NIR exposure for different time durations. (Adapted from Ref. [136].) (B) Schematic diagram of pH-triggered drug release tracking in acidic conditions by monitoring the SERS and fluorescence signal from the Dox molecules. (Adapted from Ref. [137].) (C) Mechanism of dual-mode monitoring of drug release and synergistic photothermal chemotherapy under a single NIR light. (Adapted from Ref. [138].)

for NIR-triggered drug release; (ii) LRET donor-acceptor pair of the UCNP and Dox for monitoring NIR-controlled drug release by UCL signals; and (iii) anti-cancer drug residing in the hollow cavity for monitoring NIR-controlled drug release by MR signals due to the diffusion of water molecules from outside to the Gd-UCNP core. *In vitro* and *in vivo* experiments demonstrated that the Gd-UCNP cores could serve as robust nanosensors to visualize and quantify drug release in HeLa cells, zebrafish embryos, and Walker-256 tumor-bearing Sprague-Dawley rats. Shen et al. [139] proposed a dual-mode imaging and real-time monitoring strategy with photoluminescence and MRI. Two-photon-sensitized multi-functional nanospheres were developed *via* stepwise modification of hollow Gd_2O_3:Eu^{3+} nanoparticles with P(NIPAm-*co*-MAA), 4,4,4-trifluoro-1-(9-pentylcarbazole-3-yl)-1,3-butanedione anion (THA), and amine-functionalized cRGD (designated as TPNPs@cRGD). In the TPNPs@cRGD nanospheres, the photoluminescence signals of Eu^{3+} and the MR signals of Gd^{3+} were stabilized and enhanced, respectively, by the loaded drug *via* a coordination effect, while displaying excellent linear decreases upon drug release.

5.2 Fluorescence- and Raman-based multi-mode drug release monitoring system

The combination of fluorescence and Raman imaging has also been used for drug release monitoring. Kang et al. [137] presented a strategy based on plasmonic-tunable Raman/fluorescence imaging spectroscopy to track the release and delivery of an anti-cancer drug (Dox) from Au NP carriers at the single living cell level (Figure 9B). The pH-responsive drug release profile was attained through the conjugation of Dox to the nanoparticle surface *via* a pH-sensitive hydrazone linkage. When Dox was bound to the surface of Au NPs, its SERS signal was enhanced but its fluorescence was quenched. In turn, once Dox was released from Au NPs in acidic lysosomes, its Raman enhancement was greatly reduced and the Raman spectrum was changed; meanwhile, the fluorescence signal was recovered. The plasmonic-tunable Raman/fluorescence properties enabled the tracking of Dox release from the Au NP surface in living cells, and this system showed great potential in the investigation of the molecular mechanisms of drug delivery and release, as well as the cellular response to drug action.

Cao et al. [140] utilized a Janus particle with opposing mesoporous silica (MS) and gold faces for monitoring intracellular dual-drug (Dox and 6MP) release in real time based on FRET and SERS. The FRET acceptor Dox was attached to the donor 7-hydroxycoumarin-3-carboxylate (CMR)-conjugated MS with a pH-responsive linker hydrazone, and 6MP was conjugated to the gold surface through the gold-thiol interaction. The pH-triggered Dox release and GSH-responsive 6MP release were monitored according to the change of the CMR fluorescence signal and the decrease of 6MP SERS signal, respectively. This dual-drug system provided new perspectives for the real-time study of multi-drug delivery and release.

5.3 Fluorescence- and photothermal-based multi-mode drug release monitoring system

By utilizing drug-coordinated Eu^{3+} as a blocker to inhibit LRET from the Eu^{3+} complex to gold nanotriangles, multiple functions were integrated into one nanocomposite, such as operating under single NIR light, dual-mode monitoring of light-triggered drug release by photothermal imaging and two-photon luminescence imaging, and achieving synergistic photothermal chemotherapy [138] (Figure 9C). In this nanocomposite, Zhang et al. chose a two-photon-sensitized Eu^{3+} complex [$Eu(THA)_3(phen)$] as the LRET donor, gold nanotriangles as the acceptor, and a model drug (Dox) as the LRET blocker. The NIR light-mediated LRET enabled the dual-mode real-time monitoring of drug release as well as synergistic activation of multiple therapeutic potencies.

6 Conclusions and outlook

In this review, we discussed recent advances in drug release monitoring, including the strategies based on fluorescence imaging, MRI, SERS imaging, and multi-mode imaging. By comprehensively using a plethora of nanomaterials, these strategies could produce a signal response to drug release triggered by different stimuli, such as pH changes, enzymatic cleavage, redox, light, etc. Although a lot of advancements have been achieved in recent years, this field is still in its infancy and more research efforts are still desired in the future.

(i) At present, most drug release monitoring strategies are limited to qualitative determination. Developing new strategies for precise quantitative detection of drug release, especially *in vivo*, is urgently needed for accurately reflecting the relationship between drug release and treatment effect. Although many ratiometric methods have been developed thus far, few

examples have had success in precise quantitative detection of drug release because their poor accuracy and precision are mainly hampered by the imaging sensitivity and resolution. In this regard, it would be helpful to construct novel functional nanoprobes with intriguing properties to improve the spatiotemporal resolution and sensitivity of imaging, improve the resolution of the instruments, or integrate multiple imaging contrast agents with different signal outputs.

(ii) The ability to complete multiple tasks, such as drug release monitoring, tumor microenvironment imaging, and treatment effect assessment, in one platform is desired for understanding the interaction among drug release, tumor microenvironment variation, and treatment effect. Developing nanomaterial-based contrast agents that possess smart, activatable, multi-responsive criteria is an appealing direction. For instance, if an agent can selectively change its generated signal amplitude or spectrum parameters along with different stimuli, it may respond to multiple biological events simultaneously. Alternatively, if the agent with different functional groups can be modified in response to different stimuli, the designed system can be used as an indicator of multiple functional parameters to reflect various physiological/pathological status and visualize multiple events separately.

(iii) Considering that each imaging modality has its inherent pros and cons, the successful use of non-invasive imaging techniques is highly dependent on the choice of the right imaging modality and the right contrast agent. To accurately and quantitatively monitor the drug release, sometimes only one imaging modality is needed; however, in most cases, a combination of two or more different imaging techniques is required. Thus far, fluorescence imaging, MRI, and SERS are the most promising techniques, but the future exploration should not be limited to them. For example, there are some other burgeoning non-invasive imaging techniques, such as ultrasound imaging (USI), photoacoustic imaging (PAI), and optical coherence tomography (OCT), which hold great promise for monitoring drug release.

USI is based on the principle that the backscattered signals from acoustic waves vary depending on reflection by different tissues or ultrasound (US) contrast agents (i.e. gas- or air-filled micro/nanobubbles). US can convey a clear anatomical depiction of the tissue of interest, with high temporal and spatial resolution. In recent years, the US technique has been used for drug delivery by combining with microbubble- and nanobubble-based formulations, which can be either co-loaded with drugs or administered separately, to enhance extravasation, penetration, or cellular internalization and non-invasively track the fate of micro-/nanobubbles. Besides for imaging, US can also be used for therapeutic purposes by increasing the tissue temperature to 70°C for ablation with HIFU, or induce mild hyperthermia to change the carriers to release drugs with low-intensity.

PAI synergistically combines optical and USI technologies, and possesses high spatial resolution and deep tissue penetration. It is based on the photoacoustic effect that the optical absorption from non-ionizing laser pulses will be converted into heat, leading to transient thermoelastic expansion and thus wideband ultrasonic emission that is recorded by ultrasonic transducers to produce a 3D image. The emergence of various contrast agents such as organic chromophores (BHQ3, Cy5.5, Alexa 750, etc.) or inorganic nanoparticles (AuNRs, carbon nanoparticles, copper sulfide nanoparticles, etc.) with high NIR absorbance greatly accelerated the applications of PAI in tumor imaging and carrier tracking.

OCT can use the interference of light to generate two-dimensional cross-sectional images. Similar to USI techniques, OCT receives optical backscattered signal from the sample instead of an acoustic wave, enabling non-invasive acquisition of 2D/3D microstructures of biological tissue without extra contrast agents. In contrast, OCT can achieve a resolution as high as 1–10 μm, which is 1–2 orders of magnitude higher than that of USI, and a deep imaging at 2–3 mm compared with microscope-based techniques. Because of the features of non-invasive scanning, high imaging speed, and label-free imaging, OCT has been widely used in the biomedical fields, such as ophthalmology, cardiac diseases, dermatology, and cancer.

Although some of the techniques have been applied in clinical trials, their applications in drug release monitoring remains unexplored, possibly because of the poor resolution, high cost of the instruments, or lack of ideal imaging agents. Thus, it is highly promising to design multi-mode imaging agents using functional nanomaterials to make the most use of different imaging techniques, thus providing accurate, real-time, and *in situ* information to facilitate the translation of nanomedicine in treating human disease.

Acknowledgments: This research was supported by the Natural Science Foundation of Jiangsu Province (Funder Id: http://dx.doi.org/10.13039/501100004608, BK20180974, BK20170571) and the National Natural Science Foundation of China (Funder Id: http://dx.doi.org/10.13039/501100001809, nos. 21804059, 2170010150).

References

[1] Atkins JH, Gershell LJ. Selective anticancer drugs. Nat Rev Cancer 2002;2:645–6.

[2] Hubbell JA, Langer R. Translating materials design to the clinic. Nat Mater 2013;12:963–6.

[3] Mura S, Nicolas J, Couvreur P. Stimuli-responsive nanocarriers for drug delivery. Nat Mater 2013;12:991–1003.

[4] Wu XM, Zhu WH. Stability enhancement of fluorophores for lighting up practical application in bioimaging. Chem Soc Rev 2015;44:4179–84.

[5] Duncan R, Sat YN. Tumour targeting by enhanced permeability and retention (EPR) effect. Ann Oncol 1998;9:39–9.

[6] Maeda H, Wu J, Sawa T, Matsumura Y, Hori K. Tumor vascular permeability and the EPR effect in macromolecular therapeutics: a review. J Control Release 2000;65:271–84.

[7] Seymou LW, Miyamoto Y, Maeda H, et al. Influence of molecular-weight on passive tumor accumulation of a soluble macromolecular drug carrier. Eur J Cancer 1995;31:766–70.

[8] Matsumura Y, Maeda H. A new concept for macromolecular therapeutics in cancer chemotherapy: mechanism of tumoritropic accumulation of proteins and the antitumor agent smancs. Cancer Res 1986;46:6387–92.

[9] Thanki K, Kushwah V, Jain S. Recent advances in tumor targeting approaches. In: Targeted drug delivery: concepts and design. Devarajan PV, Jain S, eds. Springer International Publishing, New York, 2015;2:41–112.

[10] Steichen SD, Caldorera-Moore M, Peppas NA. A review of current nanoparticle and targeting moieties for the delivery of cancer therapeutics. Eur J Pharm Sci 2013;48:416–27.

[11] Frasconi M, Liu Z, Lei J, et al. Photoexpulsion of surface-grafted ruthenium complexes and subsequent release of cytotoxic cargos to cancer cells from mesoporous silica nanoparticles. J Am Chem Soc 2013;135:11603–13.

[12] Sun J, Li Y, Chen C, et al. Magnetic Ni/Fe layered double hydroxides nanosheets as enhancer for DNA hairpin sensitive detection of miRNA. Talanta 2018;187:265–71.

[13] Chen KJ, Liang HF, Chen HL, et al. A thermoresponsive bubble-generating liposomal system for triggering localized extracellular drug delivery. ACS Nano 2013;7:438–46.

[14] Thomas CR, Ferris DP, Lee JH, et al. Noninvasive remote-controlled release of drug molecules in vitro using magnetic actuation of mechanized nanoparticles. J Am Chem Soc 2010;132:10623–5.

[15] Ruiz-Hernández E, Baeza A, Vallet-Regí M. Smart drug delivery through DNA/magnetic nanoparticle gates. ACS Nano 2011;5:1259–66.

[16] Rapoport NY, Kennedy AM, Shea JE, Scaife CL, Nam KH. Controlled and targeted tumor chemotherapy by ultrasound-activated nanoemulsions/microbubbles. J Control Release 2009;138:268–76.

[17] Schroeder A, Goldberg MS, Kastrup C, et al. Remotely activated protein-producing nanoparticles. Nano Lett 2012;12:2685–9.

[18] Xiao Z, Ji CW, Shi JJ, et al. DNA self-assembly of targeted near-infrared- responsive gold nanoparticles for cancer thermo-chemotherapy. Angew Chem Int Ed 2012;54:11853–7.

[19] Yan Q, Yuan JY, Cai, ZN, et al. Voltage-responsive vesicles based on orthogonal assembly of two homopolymers. J Am Chem Soc 2010;132:9268–70.

[20] Kim H, Jeong SM, Park JW. Electrical switching between vesicles and micelles via redox-responsive self-assembly of amphiphilic rod-coils. J Am Chem Soc 2011;133:5206–9.

[21] Karve S, Bandekar A, Ali MR, Sofou S. The pH-dependent association with cancer cells of tunable functionalized lipid vesicles with encapsulated doxorubicin for high cell-kill selectivity. Biomaterials 2010;31:4409–16.

[22] Du JZ, Du XJ, Mao CQ, Wang J. Tailor-made dual pH-sensitive polymer-doxorubicin nanoparticles for efficient anticancer drug delivery. J Am Chem Soc 2011;133:17560–3.

[23] Kim H, Kim S, Park C, et al. Glutathione-induced intracellular release of guests from mesoporous silica nanocontainers with cyclodextrin gatekeepers. Adv Mater 2010;22:4280–3.

[24] Kurtoglu YE, Navath RS, Wang B, et al. Poly(amidoamine) dendrimer-drug conjugates with disulfide linkages for intracellular drug delivery. Biomaterials 2009;30:2112–21.

[25] Zhu L, Kate P, Torchilin VP. Matrix metalloprotease 2-responsive multifunctional liposomal nanocarrier for enhanced tumor targeting. ACS Nano 2012;6:3491–8.

[26] Bernardos A, Mondragon L, Aznar E, et al. Enzyme-responsive intracellular controlled release using nanometric silica mesoporous supports capped with “saccharides”. ACS Nano 2010;4:6353–68.

[27] Kelkar SS, Reineke TM. Theranostics: combining imaging and therapy. Bioconjug Chem 2011;22:1879–903.

[28] Ryu JH, Lee S, Son S, et al. Theranostic nanoparticles for future personalized medicine. J Control Release 2014;190:477–84.

[29] Lim EK, Kim T, Paik S, et al. Nanomaterials for theranostics. Chem Rev 2014;115:327–94.

[30] Louie A. Multimodality imaging probes: design and challenges. Chem Rev 2010;110:3146–95.

[31] MacKay JA, Li Z. Theranostic agents that co-deliver therapeutic and imaging agents. Adv Drug Deliv Rev 2010;62:1003–4.

[32] Janib SM, Moses AS, MacKay JA. Imaging and drug delivery using theranostic nanoparticles. Adv Drug Deliv Rev 2010;62:1052–63.

[33] Chen X, Gambhir SS, Cheon J. Theranostic nanomedicine. Acc Chem Res 2011;44:841–1.

[34] Shen W, Li Y, Qi T, et al. Fluorometric determination of zinc(II) by using DNAzyme-modified magnetic microbeads. Microchim Acta 2018;185:447.

[35] Licha K, Olbrich C. Optical imaging in drug discovery and diagnostic applications. Adv Drug Deliv Rev 2005;57:1087–108.

[36] Mountz JM, Alavi A, Mountz JD. Emerging optical and nuclear medicine imaging methods in rheumatoid arthritis. Nat Rev Rheumatol 2012;8:719–28.

[37] Ntziachristos V, Breme C, Weissleder R. Fluorescence imaging with near-infrared light: new technological advances that enable in vivo molecular imaging. Eur J Radiol 2003;13:195–208.

[38] Kumar S, Richards-Kortum R. Optical molecular imaging agents for cancer diagnostics and therapeutics. Nanomedicine 2011;1:23–30.

[39] Weinstain R, Segal E, Satchi-Fainaro R, Shabat D. Real-time monitoring of drug release. Chem Commun 2010;46:553–5.

[40] Bazylevich A, Patsenker LD, Gellerman G. Exploiting fluorescein based drug conjugates for fluorescent monitoring in drug delivery. Dyes Pigments 2017;139:460–72.

[41] Hu YY, Zeng F. A theranostic prodrug based on FRET for real-time release monitoring in response to biothiols. Mater Sci Eng C 2017;72:77–85.

[42] Liu Y, Pei Q, Li ZS, et al. Reduction-responsive fluorescence off-on BODIPY-camptothecin conjugates for self-reporting drug release. J Mater Chem B 2016;4:2332–7.
[43] Liu PL, Xu JS, Yan DG, et al. A DT-diaphorase responsive theranostic prodrug for diagnosis, drug release monitoring and therapy. Chem Commun 2015;51:9567–70.
[44] Li BW, Liu PL, Yan DG, et al. A self-immolative and DT-diaphorase-activatable prodrug for drug-release tracking and therapy. J Mater Chem B 2017;5:2635–43.
[45] Kong XQ, Dong BL, Song XZ, et al. Dual turn-on fluorescence signal-based controlled release system for real-time monitoring of drug release dynamics in living cells and tumor tissues. Theranostics 2018;8:800–11.
[46] Zhang YF, Yin Q, J Yen, et al. Non-invasive, real-time reporting drug release in vitro and in vivo. Chem Commun 2015;51:6948–51.
[47] Wu XM, Sun XR, Guo ZQ, et al. In vivo and in situ tracking cancer chemotherapy by highly photostable NIR fluorescent theranostic prodrug. J Am Chem Soc 2014;136:3579–88.
[48] Ye MZ, Wang XH, Tang JB, et al. Dual-channel NIR activatable theranostic prodrug for in vivo spatiotemporal tracking thiol-triggered chemotherapy. Chem Sci 2016;7:4958–65.
[49] Liu PL, Li BW, Zhan CY, et al. A two-photon-activated prodrug for therapy and drug release monitoring. J Mater Chem B 2017;5:7538–46.
[50] Li SY, Liu LH, Rong LF, et al. A dual-FRET-based versatile prodrug for real-time drug release monitoring and in situ therapeutic efficacy evaluation. Adv Funct Mater 2015;25:7317–26.
[51] Jana A, Devi KS, Maiti TK, et al. Perylene-3-ylmethanol: fluorescent organic nanoparticles as a single-component photoresponsive nanocarrier with real-time monitoring of anticancer drug release. J Am Chem Soc 2012;134:7656–9.
[52] Jana A, Nguyen KT, Li X, et al. Perylene-derived single-component organic nanoparticles with tunable emission: efficient anticancer drug carriers with real-time monitoring of drug Release. ACS Nano 2014;86:5939–52.
[53] Shiran F, Hemda BC, Rachel B, et al. Polymeric nanotheranostics for real-time non-invasive optical imaging of breast cancer progression and drug release. Cancer Lett 2014;352:81–9.
[54] Zhang JF, Li SL, Liu J, et al. Self-carried curcumin nanoparticles for in vitro and in vivo cancer therapy with real-time monitoring of drug release. Nanoscale 2015;7:13503–10.
[55] Wu WC, Chang HH. Fluorescent polymeric micelles containing fluorine derivatives for monitoring drug encapsulation and release. Colloid Polym Sci 2015;293:453–62.
[56] Reichel D, Rychahou P, Bae Y. Polymer nanoassemblies with solvato- and halo- fluorochromism for drug release monitoring and metastasis imaging. Ther Deliv 2015;6:1221–37.
[57] Aibani N, Da Costa PF, Masterson J, et al. The integration of triggered drug delivery with real time quantification using FRET; creating a super 'smart' drug delivery system. J Control Release 2017;264:136–44.
[58] Liow SS, Dou Q, Kai D, et al. Long-term real-time in vivo drug release monitoring with AIE thermogelling polymer. Small 2017;13:1603404.
[59] Cao SP, Pei ZC, Xu YQ, et al. Glyco-nanovesicles with activatable near-infrared probes for real-time monitoring of drug release and targeted delivery. Chem Mater 2016;28:4501–6.
[60] Yan CX, Guo ZQ, Liu YJ, et al. A sequence-activated and logic dual-channel fluorescent probe for tracking programmable drug release. Chem Sci 2018;9:6176–82.
[61] Yang Y, Song QS, Gao K, et al. LaF_3:Eu^{3+} nanocrystal/PNIPAM nanogels: preparation, thermosensitive fluorescence performance and use as bioprobes for monitoring drug release. J Appl Polym Sci 2014;131:39930–7.
[62] Han K, Zhang WY, Zhang J, et al. pH-responsive nanoscale coordination polymer for efficient drug delivery and real-time release monitoring. Adv Healthc Mater 2017;1700470–8.
[63] Fan Z, Sun L, Huang Y, et al. Bioinspired fluorescent dipeptide nanoparticles for targeted cancer cell imaging and real-time monitoring of drug release. Nat Nanotechnol 2016;11:388–94.
[64] Lai JP, Shah BP, Garfunkel E, et al. Versatile fluorescence resonance energy transfer-based mesoporous silica nanoparticles for real-time monitoring of drug release. ACS Nano 2013;7:2741–50.
[65] Lai CY, Trewyn BG, Jeftinija DM, et al. A mesoporous silica nanosphere-based carrier system with chemically removable CdS nanoparticle caps for stimuli-responsive controlled release of neurotransmitters and drug molecules. J Am Chem Soc 2003;125:4451–59.
[66] Chen PJ, Hu SH, Hsiao CS, et al. Multifunctional magnetically removable nanogated lids of Fe_3O_4 capped mesoporous silica nanoparticles for intracellular controlled release and MR imaging. J Mater Chem 2011;21:2535–43.
[67] Vivero-Escoto JL, Slowing II, Wu CW, et al. Photoinduced intracellular controlled release drug delivery in human cells by gold-capped mesoporous silica nanosphere. J Am Chem Soc 2009;131:3462–3.
[68] Muharnmad F, Guo M, Qi W, et al. pH-triggered controlled drug release from mesoporous silica nanoparticles via intracellular dissolution of ZnO nanolids. J Am Chem Soc 2011;133:8778–81.
[69] Chen T, Yu H, Yang NW, et al. Graphene quantum dot-capped mesoporous silica nanoparticles through an acid-cleavable acetal bond for intracellular drug delivery and imaging. J Mater Chem B 2014;2:4979–82.
[70] Zhu Y, Meng W, Gao H, et al. Hollow mesoporous silica/poly(L-lysine) particles for codelivery of drug and gene with enzyme-triggered release property. J Phys Chem C 2011;115:13630–6.
[71] Climent E, Martnez-Manez R, Sancenon F, et al. Controlled delivery using oligonucleotide-capped mesoporous silica nanoparticles. Angew Chem Int Ed 2010;49:7281–83.
[72] Chen C, Geng J, Pu F, et al. Polyvalent nucleic acid/mesoporous silica nanoparticle conjugates: dual stimuli-responsive vehicles for intracellular drug delivery. Angew Chem Int Ed 2011;50:882–86.
[73] Wu S, Huang X, Du X. Glucose and pH responsive controlled release of cargo from protein gated carbohydrate-functionalized mesoporous silica nanocontainers. Angew Chem Int Ed 2013;52:1–6.
[74] Wang R, Zhou L, Wang WX, et al. In vivo gastrointestinal drug-release monitoring through second near-infrared window fluorescent bioimaging with orally delivered microcarriers. Nat Commun 2017;8:14702.
[75] Valetti S, Wankar J, Ericson MB, et al. Mesoporous silica particles as a lipophilic drug vehicle investigated by fluorescence lifetime imaging. J Mater Chem B 2017;5:3201–11.

[76] Chen HY, Moore T, Qi B, et al. Monitoring pH-triggered drug release from radioluminescent nanocapsules with X-ray excited optical luminescence. ACS Nano 2013;7:1178–87.
[77] Lee J, Jeong C, Kim WJ. Facile fabrication and application of near-IR light-responsive drug release system based on gold nanorods and phase change material. J Mater Chem B 2014;2:8338–45.
[78] Shan CF, Wang BK, Hu BB, et al. Smart yolk-shell type luminescent nanocomposites based on rare-earth complex for NIR-NIR monitor of drug release in chemotherapy. J Photochem Photobiol A 2018;355:233–41.
[79] Baggaley E, Botchway SW, Haycock JW, et al. Long-lived metal complexes open up microsecond lifetime imaging microscopy under multiphoton excitation: from FLIM to PLIM and beyond. Chem Sci 2014;5:879.
[80] Ma Y, Liang H, Zeng Y, et al. Phosphorescent soft salt for ratiometric and lifetime imaging of intracellular pH variations. Chem Sci 2016;7:3338–46.
[81] Itoh H, Arai S, Sudhaharan T, et al. Direct organelle thermometry with fluorescence lifetime imaging microscopy in single myotubes. Chem Commun 2016;52:4458–61.
[82] Sun YP, Zhou B, Lin Y, et al. Quantum-sized carbon dots for bright and colorful photoluminescence. J Am Chem Soc 2006;128:7756–7.
[83] Kong B, Zhu A, Ding C, et al. Carbon dot-based inorganic-organic nanosystem for two-photon imaging and biosensing of pH variation in living cells and tissues. Adv Mater 2012;24:5844–8.
[84] Goh EJ, Kim KS, Kim YR, et al. Bioimaging of hyaluronic acid derivatives using nanosized carbon dots. Biomacromolecules 2012;13:2554–61.
[85] Zhu S, Meng Q, Wang L, et al. Highly photoluminescent carbon dots for multicolor patterning, sensors, and bioimaging. Angew Chem Int Ed 2013;52:3953–7.
[86] Tang J, Kong B, Wu H, et al. Carbon nanodots featuring efficient FRET for real-time monitoring of drug delivery and two-photon imaging. Adv Mater 2013;25:6569–74.
[87] Paul A, Jana A, Sambath K, et al. Photoresponsive real time monitoring silicon quantum dots for regulated delivery of anticancer drugs. J Mater Chem B 2016;4:521–8.
[88] Zheng FF, Zhang PH, Xi Y, et al. Aptamer/graphene quantum dots nanocomposite capped fluorescent mesoporous silica nanoparticles for intracellular drug delivery and real-time monitoring of drug release. Anal Chem 2015;87:11739–45.
[89] Peng F, Su Y, Zhong Y, et al. Silicon nanomaterials platform for bioimaging, biosensing, and cancer therapy. Acc Chem Res 2014;47:612–23.
[90] Ohta S, Shen P, Inasawa S, et al. Size and surface chemistry-dependent intracellular localization of luminescent silicon quantum dot aggregates. J Mater Chem 2012;22:10631–8.
[91] Tu C, Ma X, Pantazis P, et al. Paramagnetic, silicon quantum dots for magnetic resonance and two-photon imaging of macrophages. J Am Chem Soc 2010;132:2016–23.
[92] Zhong Y, Peng F, Wei X, et al. Microwave-assisted synthesis of biofunctional and fluorescent silicon nanoparticles using proteins as hydrophilic ligands. Angew Chem Int Ed 2012;51:8485–9.
[93] Hessel CM, Rasch MR, Hueso JL, et al. Alkyl passivation and amphiphilic polymer coating of silicon nanocrystals for diagnostic imaging. Small 2010;6:2026–34.
[94] Tu C, Ma X, House A, et al. PET imaging and biodistribution of silicon quantum dots in mice. ACS Med Chem Lett 2011;2:285–8.
[95] Wang Q, Bao Y, Ahire J, et al. Co-encapsulation of biodegradable nanoparticles with silicon quantum dots and quercetin for monitored delivery. Adv Healthc Mater 2013;2:459–66.
[96] Hanada S, Fujioka K, Futamura Y, et al. Evaluation of anti-inflammatory drug-conjugated silicon quantum dots: their cytotoxicity and biological effect. J Mol Sci 2013;14:1323–34.
[97] Ohta S, Yamura K, Inasawa S, et al. Aggregates of silicon quantum dots as a drug carrier: selective intracellular drug release based on pH-responsive aggregation/dispersion. Chem Commun 2015;51:6422–5.
[98] Cao F, Ju E, Liu C, et al. Encapsulation of aggregated gold nanoclusters in a metal-organic framework for real-time monitoring of drug release. Nanoscale 2017;9:4128–34.
[99] Yan X, Li BS, Li LS. Colloidal graphene quantum dots with well-defined structures. Acc Chem Res 2013;46:2254–62.
[100] Li LL, Wu GH, Yang GH, et al. Focusing on luminescent graphene quantum dots: current status and future perspectives. Nanoscale 2013;5:4015–39.
[101] Liu Y, Song N, Ma Z, et al. Synthesis of a poly(N-methylthionine)/reduced graphene oxide nanocomposite for the detection of hydroquinone. Mater Chem Phys 2019;223:548–56.
[102] Chen C, Gan Z, Zhou K, et al. Catalytic polymerization of N-methylthionine at electrochemically reduced graphene oxide electrodes. Electrochim Acta 2018;283:1649–59.
[103] Bansal A, Zhang, Y. Photocontrolled nanoparticle delivery systems for biomedical applications. Acc Chem Res 2014;47:3052–60.
[104] Yang YM. Upconversion nanophosphors for use in bioimaging, therapy, drug delivery and bioassays. Microchim Acta 2014;181:263–94.
[105] Nguyen PD, Son SJ, Min J. Upconversion nanoparticles in bioassays, optical imaging and therapy. J Nanosci Nanotechnol 2014;14:157–74.
[106] Chen F, Bu W, Cai W, Shi J. Functionalized upconversion nanoparticles: versatile nanoplatforms for translational research. Curr Mol Med 2013;13:1613–32.
[107] Lai JP, Zhang YX, Pasquale N, Lee KB. An upconversion nanoparticle with orthogonal emissions using dual NIR excitations for controlled two-way photoswitching. Angew Chem Int Ed 2014;53:14419–23.
[108] Chen GY, Qiu HL, Prasad PN, Chen XY. Upconversion nanoparticles: design, nanochemistry, and applications in theranostics. Chem Rev 2014;114:5161–214.
[109] Wang FF, Zhai D, Wu C, Chang J. Multifunctional mesoporous bioactive glass/upconversion nanoparticle nanocomposites with strong red emission to monitor drug delivery and stimulate osteogenic differentiation of stem cells. Nano Res 2016;9:1193–208.
[110] Li K, Su Q, Yuan W, et al. Ratiometric monitoring of intracellular drug release by an upconversion drug delivery nanosystem. ACS Appl Mater Interfaces 2015;7:12278–86.
[111] Lai JP, Shah BP, Zhang YX, et al. Real-time monitoring of ATP-responsive drug release using mesoporous-silica-coated multicolor upconversion nanoparticles. ACS Nano 2015;95:5234–45.
[112] Mulder WJ, McMahon MT, Nicolay K. The evolution of MRI probes: from the initial development to state-of-the-art applications. NMR Biomed 2013;26:725–7.

[113] Langereis S, Geelen T, Grull H, et al. Paramagnetic liposomes for molecular MRI and MRI-guided drug delivery. NMR Biomed 2013;26:728–44.
[114] Kluza E, Strijkers GJ, Nicolay K. Multifunctional magnetic resonance imaging probes. Recent Results Cancer Res 2013;187:151–90.
[115] Caravan P, Ellison JJ, McMurry TJ, Lauffer RB. Gadolinium(III) chelates as MRI contrast agents: structure, dynamics, and applications. Chem Rev 1999;8:2293–352.
[116] Klasson A, Ahren M, Hellqvist E, et al. Positive MRI contrast enhancement in THP-1 cells with Gd_2O_3 nanoparticles. Contrast Media Mol Imaging 2008;3:106–11.
[117] Zhang Y, Lin JD, Vijayaragavan V, et al. Tuning sub-10 nm single-phase $NaMnF_3$ nanocrystals as ultrasensitive hosts for pure intense fluorescence and excellent T1 magnetic resonance imaging. Chem Commun 2012;48:10322–24.
[118] Weissleder R, Elizondo G, Wittenberg J, et al. Ultrasmall supermagnetic iron oxide: characterization of a new class of contrast agents for MR imaging. Radiology 1990;175:489–93.
[119] Frey NA, Peng S, Cheng K, et al. Magnetic nanoparticles: synthesis, functionalization, and applications in bioimaging and magnetic energy storage. Chem Soc Rev 2009;38:2532–42.
[120] Terreno E, Castelli DD, Viale A, et al. Challenges for molecular magnetic resonance imaging. Chem Rev 2010;110:3019–42.
[121] He Z, Zhang PH, Xiao Y, et al. Acid-degradable gadolinium-based nanoscale coordination polymer: a potential platform for targeted drug delivery and potential magnetic resonance imaging. Nano Res 2018;11:929–39.
[122] Cai XJ, Gao W, Ma M, et al. A Prussian blue-based core-shell hollow-structured mesoporous nanoparticle as a smart theranostic agent with ultrahigh pH-responsive longitudinal relaxivity. Adv Mater 2015;27:6382–9.
[123] Kaittanis C, Shaffer TM, Bolaender A, et al. Multifunctional MRI/PET nanobeacons derived from the in situ self-assembly of translational polymers and clinical cargo through coalescent intermolecular forces. Nano Lett 2015;15:8032–43.
[124] Kim HR, You DG, Park SJ, et al. MRI monitoring of tumor-selective anticancer drug delivery with stable thermosensitive liposomes triggered by high-intensity focused ultrasound. Mol Pharm 2016;13:1528–39.
[125] Dong Z, Feng L, Zhu W, et al. $CaCO_3$ nanoparticles as an ultra-sensitive tumor-pH-responsive nanoplatform enabling real-time drug release monitoring and cancer combination therapy. Biomaterials 2016;110:60–70.
[126] Kaittanis C, Shaffer TM, Ogirala A, et al. Environment-responsive nanophores for therapy and treatment monitoring via molecular MRI quenching. Nat Commun 2014;10:3384.
[127] Fleischmann M, Hendra PJ, McQuillan AJ. Raman spectra of pyridine adsorbed at a silver electrode. Chem Phys Lett 1974;26:163–6.
[128] Bantz KC, Meyer AF, Wittenberg NJ, et al. Recent progress in SERS biosensing. Phys Chem Chem Phys 2011;13:11551–67.
[129] Abalde-Cela S, Aldeanueva-Potel P, Mateo-Mateo C, et al. Surface-enhanced Raman scattering biomedical applications of plasmonic colloidal particles. J R Soc Interface 2010;7:435–50.
[130] Huang X, El-Sayed IH, Qian W, et al. Cancer cells assemble and align gold nanorods conjugated to antibodies to produce highly enhanced, sharp, and polarized surface Raman spectra: a potential cancer diagnostic marker. Nano Lett 2007;7:1591–7.
[131] Doering WE, Piotti ME, Natan MJ, et al. SERS as a foundation for nanoscale, optically detected biological labels. Adv Mater 2007;19:3100–8.
[132] Kamra T, Zhou T, Montelius L, et al. Implementation of molecularly imprinted polymer beads for surface enhanced Raman detection. Anal Chem 2015;87:5056–61.
[133] Ock K, Jeon WI Ganbold EO, et al. Real-time monitoring of glutathione-triggered thiopurine anticancer drug release in live cells investigated by surface-enhanced Raman scattering. Anal Chem 2012;84:2172–8.
[134] Hossain MK, Cho HY, Kim KJ, et al. In situ monitoring of doxorubicin release from biohybrid nanoparticles modified with antibody and cell-penetrating peptides in breast cancer cells using surface-enhanced Raman spectroscopy. Biosens Bioelectron 2015;71:300–5.
[135] Tian FR, Conde J, Bao CC, et al. Gold nanostars for efficient in vitro and in vivo real-time SERS detection and drug delivery via plasmonic-tunable Raman/FTIR imaging. Biomaterials 2016;106:87–97.
[136] Liu JN, Bu JW, Bu WB, et al. Real-time in vivo quantitative monitoring of drug release by dual-mode magnetic resonance and upconverted luminescence imaging, Angew Chem Int Ed 2014;53:4551–5.
[137] Kang B, Afifi MM, Austin LA, et al. Exploiting the nanoparticle plasmon effect: observing drug delivery dynamics in single cells via Raman/fluorescence imaging spectroscopy. ACS Nano 2013;7:7420–7.
[138] Zhang Y, Shen TT, Zhang HL, et al. A multifunctional nanocomposite for luminescence resonance energy transfer-guided synergistic monitoring and therapy under single near infrared light. Chem Commun 2016;52:4880–3.
[139] Shen T, Zhang Y, Kirillov AM, et al. Two-photon sensitized hollow Gd_2O_3:Eu^{3+} nanocomposites for real-time dual-mode imaging and monitoring of anticancer drug release. Chem Commun 2016;52:1447–50.
[140] Cao H, Yang YH, Chen X, et al. Intelligent Janus nanoparticles for intracellular real-time monitoring of dual drug release. Nanoscale 2016;8:6754–60.